



ΕΛΛΗΝΙΚΗ
ΕΠΙΣΤΗΜΟΝΙΚΗ
ΕΤΑΙΡΕΙΑ
ΕΔΑΦΟΜΗΧΑΝΙΚΗΣ
& ΓΕΩΤΕΧΝΙΚΗΣ
ΜΗΧΑΝΙΚΗΣ

Τα Νέα

98

της Ε Ε Ε Ε Γ Μ

Αρ. 98 – ΙΑΝΟΥΑΡΙΟΣ 2017



THESSALONIKI

16TH EUROPEAN CONFERENCE ON

EARTHQUAKE ENGINEERING

18 - 21 JUNE 2018

www.16ceee.org

IMPORTANT DATES

Abstract Submission Deadline: 31 May 2017	Notification of Acceptance: 20 July 2017	Full Paper Submission: 30 November 2017
Paper Notification of Acceptance: 28 February 2018	Early Bird Registration / Final Paper Submission: 10 April 2018	Late Registration: 1 June 2018

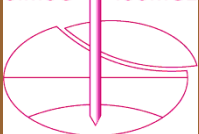
ORGANISERS



CONTACT



SIMSG ISSMGE



Π Ε Ρ Ι Ε Χ Ο Μ Ε Ν Α

16th European Conference on Earthquake Engineering	1
Η ΕΕΕΕΓΜ αποκτά προφίλ στο LinkedIn	2
Άρθρα	4
- Safety considerations for the HYD limit stat	4
- Finite element investigation of vertical stabilisation piles in a stiff clay excavated slope using a nonlocal strain softening model	8
- Numerical modelling of wave attenuation through soil	12
- Technical Note: CCR Closure and Geocomposite Drainage	17
Διακρίσεις Ελλήνων Γεωμηχανικών - Harry Poulos, 2017 OPAL winner in design	21
Νέα από Ελληνικές και Διεθνείς Γεωτεχνικές Ενώσεις	22
- Ελληνική Επιτροπή Μεγάλων Φραγμάτων: Φωτογραφικός Διαγωνισμός «Φράγματα & Ταμιευτήρες»	22
Προσεχείς Γεωτεχνικές Εκδηλώσεις:	24
- Call for Papers: In situ tests in geotechnical engineering	24
- 2nd International Symposium on Coastal and Offshore Geotechnics (ISCOG 2017) & 2nd International Conference on Geo-Energy and Geo-Environment (GeGe2017)	24
- Brownfield Risk Assessment & Remediation	25
- 11ο Συνέδριο «Ελληνική Γλώσσα και Ορολογία»	25
- 9th European Conference on Numerical Methods in Geotechnical Engineering	27
- 11th International Conference on Structural Analysis of Historical Constructions "An interdisciplinary approach"	27
- Tunnels and Underground Cities: Engineering and Innovation meet Archaeology, Architecture and Art and ITA - AITES General Assembly and World Tunnel Congress	28
Ενδιαφέροντα Γεωτεχνικά Νέα	31
- 10 of the world's greatest tunnels	31
- Submarine landslide deposits – a spectacular outcrop example from Japan	34
Ενδιαφέροντα - Σεισμοί	35
- Cardiff researcher proposes anti-tsunami concept	35
Ενδιαφέροντα - Λοιπά	36
- Η ψηλότερη γέφυρα του κόσμου	36
- Roman Arch Bridges: How much weight can they hold and how did they last so long?	36
- Elbphilharmonie: το νέο μουσικο-αρχιτεκτονικό θαύμα της Ευρώπης	37
Ηλεκτρονικά Περιοδικά	39



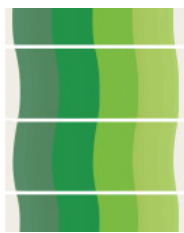
HSSMGE Greece

Hellenic Society of Soil Mechanics & Geotechnical Engineering (Greece)

Greece

Η ΕΕΕΕΓΜ αποκτά προφίλ στο LinkedIn

Η ΕΕΕΕΓΜ απέκτησε πλέον προφίλ στο δημοφιλές επαγγελματικό κοινωνικό δίκτυο LinkedIn. Σκοπός είναι η ταχύτερη και αμεσότερη πληροφόρηση για τα νέα και τις εκδηλώσεις της ΕΕΕΕΓΜ. Ήδη η ανταπόκριση των μελών μας και λοιπών ενδιαφερομένων υπήρξε σπουδαία καθώς μέσα σε μία εβδομάδα από τη δημιουργία του προφίλ περίπου 250 άτομα δημιούργησαν επαφή με το προφίλ αυτό. Όποια μέλη μας και λοιποί ενδιαφερόμενοι έχουν προφίλ στο LinkedIn και επιθυμούν να συνδεθούν με το προφίλ της ΕΕΕΕΓΜ μπορούν να στείλουν αίτημα σύνδεσης. Η επικοινωνία με τα μέλη της ΕΕΕΕΓΜ μέσω e-mail θα συνεχιστεί κανονικά όπως και σήμερα. Τονίζεται ότι η δημιουργία επαφής με το προφίλ αυτό δεν συνιστά απόκτηση ιδιότητας μέλους της ΕΕΕΕΓΜ ή της ISSMGE. Για όσους επιθυμούν κάτι τέτοιο, ισχύουν οι προβλέψεις του καταστατικού για τη διαδικασία και τις προϋποθέσεις εγγραφής στην ΕΕΕΕΓΜ.



16TH EUROPEAN CONFERENCE ON EARTHQUAKE ENGINEERING THESSALONIKI | 18 - 21 JUNE 2018

www.16ecee.org

The 16th European Conference on Earthquake Engineering, (16ECEE) will take place in Thessaloniki, Greece from 18 to 21 June 2018, organized by the Hellenic Society of Earthquake Engineering (member of EAEE), and the Civil Engineering Department of the Aristotle University of Thessaloniki.

16ECEE is around a breadth of state-of-the-art scientific topics: earthquake structural and geotechnical engineers, geologists and seismologists from all over the world will find an excellent forum to exchange ideas, share knowledge and discuss the most recent advances in soil dynamics, structural and geotechnical earthquake engineering, up to the boundaries of geology and engineering seismology.

Distinguished invited keynote lecturers will present recent and ongoing developments, addressing unresolved issues and projecting ideas for the future. Special sessions, workshops and round table discussions will also be carefully organized on selected topics of particular engineering and societal interest, to broaden the horizons of the earthquake engineering community and to reinforce international cooperation links.

The ECEE conference is a highly-anticipated event, held every four years, and is considered to be the leading activity of the European Association for Earthquake Engineering (EAEE), as well as the baseline and meeting point for the scientific and professional sector at an international level, with more than 1000 delegates from Europe and worldwide.

MORE INFORMATION www.16ecee.org

<https://www.facebook.com/16th-European-Conference-on-Earthquake-Engineering16ecee-227127680965507/>

<https://twitter.com/16ECEE?lang=en>

<https://www.linkedin.com/in/european-conference-on-earthquake-engineering256967125/>

<https://plus.google.com/u/1/109239472633725523824>

<https://www.instagram.com/16ecee/?hl=en>

IMPORTANT DATES

Abstract Submission Deadline:

31 May 2017

Notification of Acceptance:

20 July 2017

Full Paper Submission:

30 November 2017

Paper Notification of Acceptance:

28 February 2018

Early Bird Registration / Final Paper Submission

10 April 2018

Late Registration:

1 June 2018

Παρουσίαση άρθρων, στην συγγραφή των οποίων μετείχαν Έλληνες, στο XVI European Conference on Soil Mechanics and Geotechnical Engineering, Edinburgh, 13-17 September 2015 (κατ' αλφαβητική σειρά, στα ελληνικά, του ονόματος του πρώτου συγγραφέα).

Safety considerations for the HYD limit state

Considérations en matière de sécurité de l'état limite HYD

B. Simpson, G. Katsigiannis

ABSTRACT The HYD limit state, defined in Eurocode 7, relates to upward flow of water through soil to a free surface, such as may occur in front of a retaining wall in the base of an excavation. Terzaghi (1922) proposed that safety in this situation may be checked by studying the equilibrium of a rectangular block of soil extending a depth t from the free surface to the toe of the wall and of width $b=t/2$. He proposed a calculation for a factor of safety, but did not recommend a specific value for it. Many other publications have shown Terzaghi's calculation and have recommended values for the factor of safety. The range of recommended values is very large, generally with little obvious reason for such disparity. Orr (2005) discussed the application of partial factor methods to this problem, showing that the precise way they are applied may have a big effect on results, while Simpson (2012) argued that proper understanding of the concept of limit state "design values" is needed. In this paper, Terzaghi's calculation is reviewed, considering whether $b=t/2$ is a sensible prescription, what part is played by the stress state and strength of the ground and, most significantly, what is the influence of variations in permeability within the soil body. It is shown that it is far more important that designers think incisively about ground permeability than that they verify a particular factor of safety.

1 INTRODUCTION

The HYD limit state is defined in Eurocode 7 (EC7) to be related to hydraulic heave, internal erosion and piping in the ground caused by hydraulic gradients. This paper is concerned with part of this definition, hydraulic heave caused by hydraulic gradients, which is illustrated in EC7 by Figure 10.2, shown here as Figure 1.

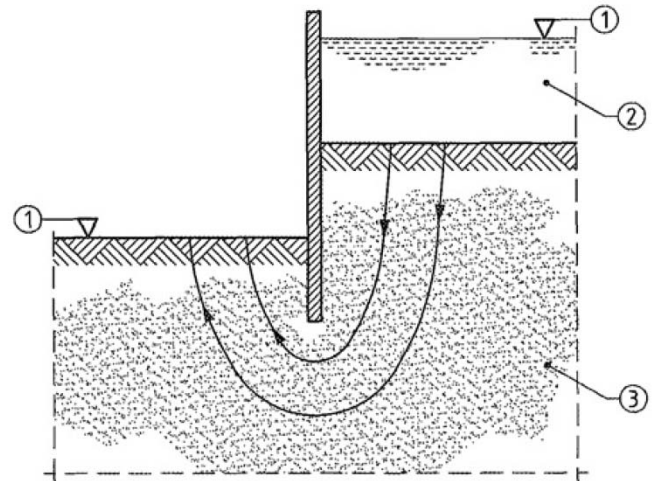
Requirements for hydraulic heave are expressed in EC7 by Equation 2.9, which has caused considerable controversy as discussed in section 3 below. Much earlier, Terzaghi (1922) proposed a calculation for this limit state, and many other publications have shown Terzaghi's calculation and have recommended values for the factor of safety. The range of recommended values is very large, generally with little obvious reason for such disparity.

Recently the problem has been discussed extensively by EC7 Evolution Group 9 on Water Pressures, and this paper draws on those discussions to develop a more pertinent approach to specification of safety for situations of hydraulic heave.

2 TERZAGHI'S CALCULATION

Terzaghi (1922) proposed that for a wall penetration t a rectangular block of soil should be considered of width $b=t/2$, as shown in Figure 2. No account is to be taken of any friction on the sides of the block at its interfaces with the wall or with the rest of the soil. Terzaghi proposed that

a factor of safety should be calculated as $FT = G'/S$, where G' is the buoyant weight of the block and S is the upwards seepage force.



1 excavation level (left); water table (right)
2 water
3 sand

Figure 1. EC7 Figure 10.2 — Example of situation where heave might be critical.

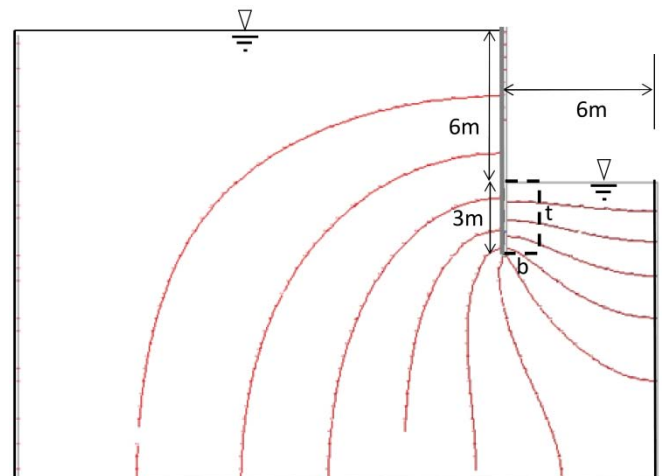


Figure 2. Terzaghi's calculation.

The authors have not been able to find any direct recommendation of Terzaghi giving a value for the required factor of safety. Terzaghi, Peck & Mesri (1996), and earlier editions of this book, give a worked example in which the acceptable factor required appears to be $F_T=2.5$. Values taken from a survey of publications and advice from European colleagues, generally based on use of Terzaghi's diagram, are summarised in Table 1. Dutch practice actually requires a factor of safety of 2.0 using a very narrow column adjacent to the wall; the factor of 2.8 shown in Table 1 is an equivalent requirement based on a column width $b=t/2$.

The values for the required factor of safety shown in Table 1 range from 1.42 to 5. While some authorities require larger factors for finer soils than for coarser soils, no explanation of this overall large range has been found. The authors speculate that it might come from the particular experiences of individual engineers working in specific geological situations. For example, it could be that those who have worked in more reliable, uniform, perhaps coarser materials have selected lower values than those who have experience

of more variable finer materials. But nothing has been found in the literature to confirm this.

Table 1. Published values for Terzaghi’s factor of safety F_T .

Publication and any limitations	Values
Williams B P & Waite D (1993) For clean sands	1.5 to 2.0
Kashef, Abdel-Aziz Ismail (1986)	4 to 5
Harr, M E. (1962)	4 to 5
German practice – unfavourable soils (DIN 1054/A2 2014) – favourable soils	1.9 1.42
Swedish practice – coarse soils (Ryner et al 1996) – silty material	1.5 2.5
Dutch practice (van Seters 2013)	2.8
Das (1983), quoting Harr (1962)	4 to 5

The International Levee Handbook (CIRIA 2103) provides a range of factors of safety for flow of water emerging from levees, though in a somewhat different form. It makes the point that the choice of factor within the range should be dependent on the consequences of failure of the levee. This is another important issue that may have influenced some of the values shown in Table 1.

3 EC7 EQUATION 2.9

EC7 represents the requirement for stability against hydraulic heave by Equation 2.9, which is presented in two forms:

$$u_{dst;d} \leq \sigma_{stb;d} \quad (2.9a)$$

$$S_{dst;d} \leq G'_{stb;d} \quad (2.9b)$$

In (2.9a) the requirement is expressed in terms of pore water pressure u and total vertical stress σ , whereas in (2.9b) it is expressed in terms of seepage force S and buoyant weight G' . Both forms of the equation use *design values* of parameters (subscript d), already incorporating safety, so no further factors are shown in the requirements. The subscripts *dst* and *stb* refer to destabilising and stabilising effects. For simple cases such as a Terzaghi’s block the two forms are mechanically equivalent provided only design values are used.

Annex A of EC7 provides values for partial factors to be used for HYD, $\gamma_{G;dst} = 1.35$ and $\gamma_{G;stb} = 0.9$. But the code does not state what quantities are to be factored. Unfortunately, some readers of EC7 have interpreted the equations to mean:

$$\gamma_{G;dst} u_{dst;k} \leq \gamma_{G;stb} \sigma_{stb;k}$$

and

$$\gamma_{G;dst} S_{dst;k} \leq \gamma_{G;stb} G'_{stb;k}$$

Here, the subscript k refers to characteristic values of the parameters. Orr (2005) pointed out that if the two equations are used in this way they can lead to markedly different results for the same values of $\gamma_{G;dst}$ and $\gamma_{G;stb}$. Simpson (2012) argued that this is a misunderstanding of the EC7 requirement, and in particular of the concept of design values, and proposed that if partial factors are to be used in this context they should be applied *excess* water pressures only, not to the hydrostatic component.

One further problem of this formulation, as with Terzaghi’s analysis, is that it is only applicable to one very specific situation of upward flow towards a horizontal surface. In practice, more complex situations are encountered, including flow beneath sloping surfaces in embankments and cuttings.

We will argue here, however, that any factoring of water pressure should be avoided.

4 STUDY FOR ISOTROPIC, HOMOGENEOUS SOIL

In all calculations presented from this point onwards, it is assumed that $\gamma = 20 \text{ kN/m}^3$ and $\gamma_w = 10 \text{ kN/m}^3$ so $\gamma/\gamma_w = 2$.

4.1 Effect of problem geometry

When water is seeping upwards beneath a narrow excavation, the upward hydraulic gradients are higher than in the case when there is no lateral restraint. To illustrate this, Figure 3 shows equipotentials for three cases: (a) a wide excavation (width $x=12t$), (b) a narrow slot ($x=t$), and (c) a circular excavation (diameter $d=t$). In each case, the seepage is supplied from a vertical boundary located 18m ($6t$) from the wall. For $\Delta h = 1.5t$, Terzaghi’s factor of safety F_T is (a) 2.89, (b) 1.33 and (c) 0.97, respectively.

This example shows that the 3D geometry of the situation is important, as has been discussed in more detail by Aulbach and Zielger (2013).

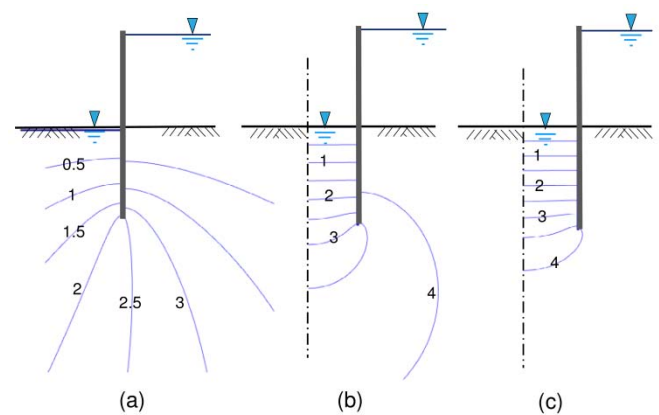


Figure 3. Equipotentials for three cases: (a) a wide excavation (width $x=12t$), (b) a narrow slot ($x=t$), and (c) a circular excavation (diameter $d=t$).

4.2 Effect of width of soil column in calculation

The remaining examples discussed in this paper will be based on the geometry shown in Figure 2. Only 2D planar seepage will be considered with an excavation wide enough to give only minor lateral restraint to the flow ($x = 4t$). Terzaghi recommended that a column of width $b=t/2$ should be used in calculations of factor of safety, taking no account of friction forces on its vertical sides. The form of the equipotentials shows, however, that the hydraulic gradient would be higher if a narrower column were used. It could be that Terzaghi considered that a narrower column is unlikely to fail because the friction forces on its vertical sides would become significant.

Figure 2 shows a situation for which Terzaghi’s calculation gives $F_T = 1.47$ ($\Delta h/t = 2$). The solid line in Figure 4 shows how the value of this factor would vary for different column widths if no account is taken of wall friction. For a material with $c'=0$, $\phi'=35^\circ$ and $\delta/\phi'=1$, a rough wall, the broken line in Figure 4 shows how the factor varies if wall friction is included in the calculation, but the block is not providing shear restraint to material further from the wall. These values depend also on other parameters such as the previous stress history, assumed here to be an excavation, and K_0 , taken here as 0.5 before excavation. For this case, the shear force on the wall is 85.1 kN/m, which increases the safety of the Terzaghi block to 4.25. For a narrow block ($b=t/6$), the shear force is almost 6 times its buoyant weight, so the factor of safety for this block becomes very large.

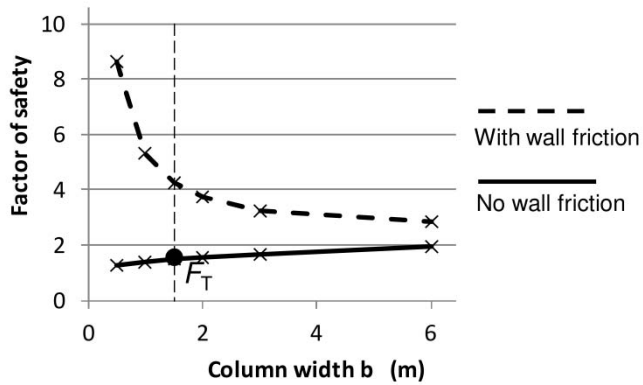


Figure 4. Significance of wall friction when $F_T = 1.47$.

For advocates of limit state design, this example raises a fundamental question: does the method require an analysis of the system for the actual design conditions required for the limit state, which could be at a point of instability, rather than calculation of a factor of safety obtained for less severe conditions? In some situations, as discussed below, it is desirable to examine the behaviour at the actual limit.

In Figure 5, the solid line shows the variation of factor of safety with column width, excluding effects of wall friction, for $\Delta h/t=3$, at which the system is close to failure, and the broken line shows the values including wall friction, which was computed as 11.5kN/m for this case. The chain-dot line shows results for $\Delta h/t=3.33$, for which the FE analysis was unstable. In this case, the pore pressures are so high that all the effective stresses have become very small, making wall friction insignificant.

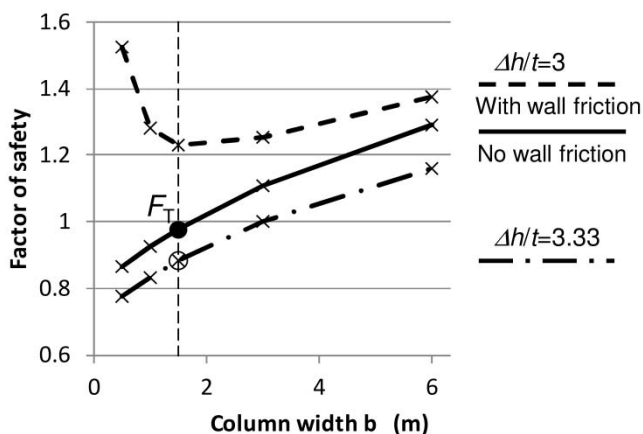


Figure 5. Significance of wall friction for F_T close to 1.0.

For this example, at least, if the Terzaghi block method ($b=t/2$) gave a factor of safety above or even marginally below unity, shear force on the wall significantly enhanced the factor. But where the factor fell significantly below unity, shear on the wall did not provide any assistance. It appears that reliance on the Terzaghi calculation to guard against the effects of potentially more adverse water pressures could be misleading and unsafe.

5 STUDY FOR HETEROGENEOUS SOILS

5.1 Reasons for factors or margins of safety

EC7 Evolution Group 9 have debated various reasons why factors of safety are needed in this situation. This relates in part to the mechanism by which failure is thought to occur, for which there are three main possibilities:

a) General heave of the ground, uplifting a large body of material.

b) A break-through in which water finds a weak path through the ground and exploits it.

c) A piping failure along the interface between the ground and a structure.

The relevant uncertainties are considered to be:

- The total or buoyant density of the soil.
- Geometric uncertainties such as ground level.
- The stress at specific points in the soil.
- The distribution of water pressure.

The total vertical stress in the ground is usually calculated as $\sigma_v = \gamma z$, where γ is total density and z is depth below the ground surface. Uncertainty of density of soil is usually fairly small, but there may be some uncertainty about depth z , especially if there is any fear of over-excavation such as formation of trenches or sumps.

It is possible, however, that hydraulic failures initiate and develop from local points in the ground or at interfaces with structures. If γ and z are well known, it could be that very locally σ_v is more variable if the ground conditions are not very uniform. This, and the previous considerations, give reason for some reduction, in design calculations, of the expected value of γz , which applies irrespective of the use of total stress or buoyant weight in the calculations.

In many situations the biggest uncertainty is likely to be the precise distribution of water pressures in the ground.

5.2 Effects of layering and anisotropy

Distribution of water pressures depends critically on the distribution and degree of anisotropy of permeability, parameters that are difficult to measure with accuracy in ground investigation tests. It is often very difficult to assess the real permeability of the ground to within a factor of 10. Figure 6 shows a series of alternative distributions of permeability in the ground, some cases also involving anisotropy. The permeabilities vary by no more than 5:1 within a depth of 3m, the wall penetration considered here. The authors consider that these variations would be difficult to identify in ground investigation, so the material could readily be classed as "uniform".

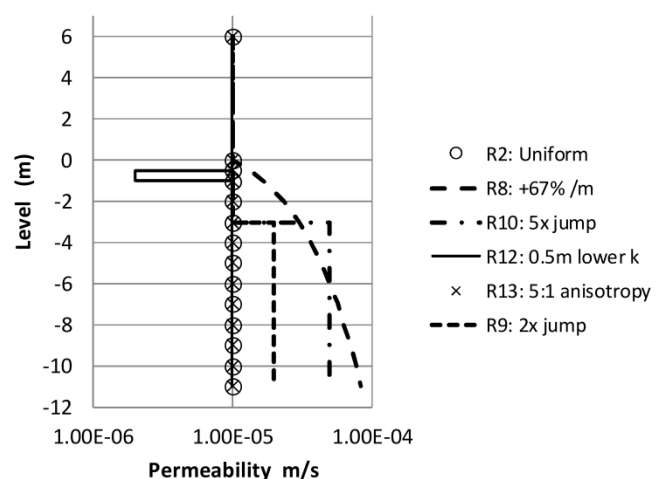


Figure 6. Distributions of permeability in the ground.

Figure 7 shows values of the ratio $F_z = G'/S$ plotted for a soil column of width $b=t/2$ and with variable depth z , plotted for $\Delta h/t=2$. This is equivalent to Terzaghi's calculation of F_T , except that this calculation is normally only carried out for depth $z=t$, the penetration of the wall.

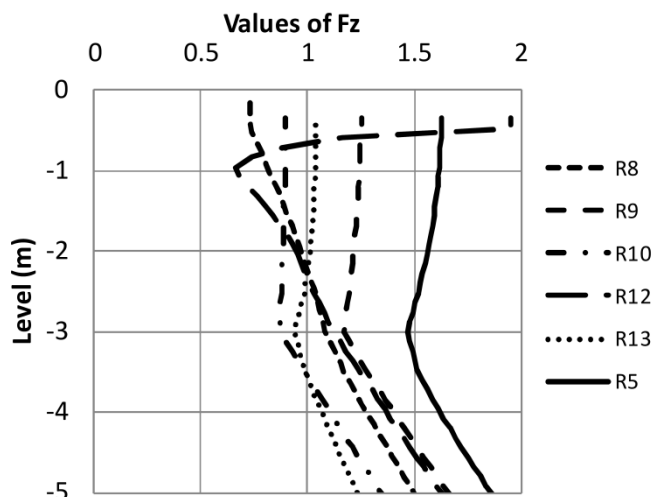


Figure 7. Values of F_z for various distributions of permeability.

For the case of homogeneous, isotropic soil (line R5), the minimum value of F_z is 1.47, occurring at $z=t$, so $F_z = F_T$. If the permeability below the wall is double that within the depth of penetration (line R9), these values fall markedly towards unity, with $F_z = F_T = 1.17$. For all the other distributions of permeability shown in Figure 6, the computations became unstable, indicating $F_z < 1$ at some depth. The minimum value of F_z does not necessarily occur at $z=t$, indicating that a failure might be initiated at a level above the bottom of the wall.

In further analyses, the excess head was reduced to 4m, giving $\Delta h/t=1.33$. For the simple isotropic case this gave a Terzaghi factor $F_T=2.08$, whereas the stepped profile of permeability R10 had only $F_T=1.27$, and the profile with a low permeability layer, R12, still had $F_z < 1$, marginally.

5.3 Implications

In the authors' opinion, the main implication of the analysis shown here is that reliance on factors of safety to accommodate uncertainties about distribution of water pressures is very unwise. Variations in permeability by factors up to 5, which could well be missed in ground investigation, can lead to drastic reductions in factors of safety and to instability. It was noted in section 2, above, that a wide range of Terzaghi's factor F_T has been recommended, without obvious rationale. Section 5.2 shows that adoption of one particular value for F_T could readily lead to unsafe designs in ground assumed, credibly but incorrectly, to be homogeneous and isotropic.

6 FUTURE DEVELOPMENTS IN EC7

Evolution Group 9 of EC7 has recommended that in situations of this type partial safety factors should not be applied to water pressures or to forces derived from water pressures, such as the seepage force S . Instead, engineers must take an appropriately cautious view of water pressures that could occur in the ground. In this case, that implies that a careful review of the possible range of distributions of permeability must be undertaken and the design must be based on the worst that is credible.

As discussed in 5.1, some allowance for uncertainty of the weight or density of the ground is relevant, though this is likely to be relatively minor.

The code requirement is then simply to prove that equilibrium exists under those design conditions. This approach has the advantage that it is fairly readily applied not only to the simple case considered in this paper, but also to more complicated situations such as water approaching sloping

ground surfaces. The verification may be made by any appropriate method, including finite element analysis or more simple calculations, if available.

It was shown in 4.2, above, that the conventional Terzaghi calculation, checking only a single column of width $b=t/2$ could be unreliable if the computed value of G/S is very close to unity or below, which could happen with the approach described here. EG9 therefore recommends that if this form of calculation is used no wall friction should be included in the calculation of equilibrium and a factor of 0.6 should be applied to the buoyant weight of the soil; this is equivalent to an effective factor of safety $F_T=1.67$.

7 CONCLUDING REMARKS

By studying a range of geometries and distributions of permeability for a simple situation, this paper shows that use of a simple calculation with reliance on a fixed factor of safety could be unsafe. Rather, it is essential that a careful review is made of the effects of possible distributions of permeability so as to derive the most adverse distribution of water pressures that is credible. Having done that, applications of further factors to water pressures or to quantities dependent on water pressures are irrelevant and are not recommended.

ACKNOWLEDGEMENT

The authors gratefully acknowledge many fruitful discussions with members of EC7 Evolution Group 9.

REFERENCES

- Aulbach, B and Zielger, M (2013) Simplified design of excavation support and shafts for safety against hydraulic heave. *Geotechnics and tunnelling*, Vol 6, August 2013, pp362-374.
- CIRIA (2013) *The International Levee Handbook*. CIRIA Report C731.
- Das, B.M. (1983) *Advanced Soil Mechanics*. McGraw-Hill.
- DIN 1054/A2 (2014) *Subsoil – Verification of the safety of earthworks and foundations – Supplementary rules to DIN EN 1997-1:2010; Amendment A2:2014*
- Harr, M E. (1962) *Groundwater and Seepage*. McGraw-Hill.
- Kashef, Abdel-Aziz Ismail (1986) *Groundwater Engineering*. McGraw Hill.
- Orr, TLL (2005) Model Solutions for Eurocode 7 Workshop Examples. Trinity College, Dublin.
- Ryner, A, Fredriksson, A and Stille, H (1996) *Sponthandboken: handbok för konstruktion och utformning av sponter*. Bygghälsningsrådet T18:1996 (ISBN 91-540-5764-7)
- Simpson, B (2012) Eurocode 7 – fundamental issues and some implications for users. Keynote lecture, *Proc 16th Nordic Geotechnical Meeting*, Vol 1, pp 29-52, Copenhagen. Danish Geotechnical Society.
- Terzaghi, K (1922) *Der Grundbuch an Stauwerken und seine Verhütung*. Forch-heimer-Nummer der Wasserkraft, p 445-449.
- Terzaghi K, Peck R B & Mesri G (1996) *Soil mechanics in engineering practice*, 3rd edition. John Wiley & Sons.
- van Seters, A. (2013) *Personal communication*.
- Williams B P & Waite D (1993) *The design and construction of sheet-piled cofferdams*. Special publication 95. Construction Industry Research and Information Association, London.

Finite element investigation of vertical stabilisation piles in a stiff clay excavated slope using a nonlocal strain softening model

Etude par la méthode des éléments finis de pieux stabilisateurs verticaux sur une pente excavée dans des sols argileux rigides à l'aide d'une modélisation non-local de l'amollissement

F.C. Summersgill, S. Kontoe and D.M. Potts

ABSTRACT Slopes excavated in stiff clay are prone to delayed and brittle failure. These slopes are widespread across the rail and road networks in the United Kingdom. The use of a row of discrete vertical piles is an established method, successfully used to remediate failure of existing slopes and to stabilise potentially unstable slopes created by widening transport corridors. This paper will challenge the assumptions made in current design procedures for these piles, which treat the pile only as an additional force or moment and simplify soil/pile interaction. Two dimensional plane-strain finite element analyses were performed to simulate the excavation of the slope in an overconsolidated clay and the interaction of vertical piles within the slope. A nonlocal strain softening model was employed for the stiff clay to reduce the mesh dependency of the solution. This model controls the development of strain by relating the surrounding strains to the calculation of strain at that point, using a weighting function. A variety of different failure mechanisms developed depending on pile location and length. The variability of the pile and slope interaction that was modelled suggests that an oversimplification during design could miss the critical failure mechanism or provide a conservative stabilisation solution. Given the prevalence of stiff clay in the UK transport infrastructure, increased capacity requirements and the age of slopes in this material, an informed and more realistic design of stabilisation piles will become increasingly necessary.

1 INTRODUCTION

Slopes excavated in stiff clay are prone to delayed and brittle failure (Potts et al. 1997). These slopes are widespread across the rail and road networks in the UK (Wilkinson et al. 2011). The use of a row of discrete vertical piles is an established stabilisation method, successfully used to remediate failure of an existing slope and to stabilize potentially unstable slopes created by widening transport corridors (Carder 2009; Ellis et al. 2010).

The current design procedures for horizontally loaded vertical stabilisation piles employ the displacements and critical slip surface of the unstabilised slope. The p-y method uses the expected soil displacements to calculate pile reaction (Baguelin et al. 1977). In a limit equilibrium or limit analysis design procedure, the pile is treated only as an additional force or moment located where the critical slip surface and pile coincide (Hassiotis et al. 1997).

These methods assume that the insertion of a pile will not affect the failure mechanism and the stabilizing effect of the pile will not be significantly affected by its position or length. The finite element method can model the pile and soil interaction in an unstable slope without a predetermined location for the slip surface. The influence of pile location and length on the slope failure mechanism can therefore be assessed.

2 FINITE ELEMENT ANALYSES

Two dimensional plane-strain finite element analyses were performed to simulate the excavation of the slope in overconsolidated clay and the interaction of vertical piles within the slope. The slope is not a specific case study, but a generic slope with dimensions known to be unstable in London Clay (Potts et al. 1997; Ellis & O'Brien, 2007). The

slope is 10m in height with a 1 in 3 vertical to horizontal slope angle (Figure 1). Soil properties for London Clay are employed (Table 1).

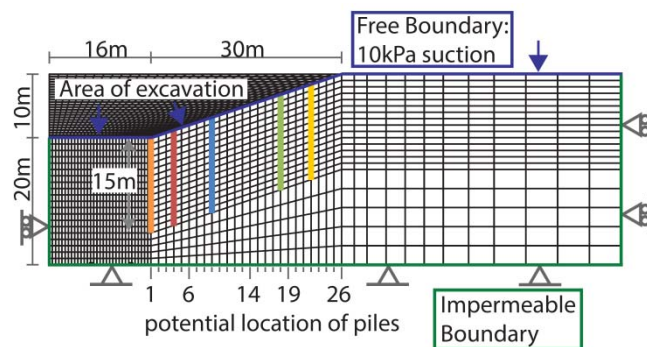


Figure 1. Finite element mesh with excavation dimensions, boundary conditions and potential pile locations.

Table 1. Soil properties for London clay excavated slope analyses.

Property	Value
Bulk unit weight	$\gamma = 18.8 \text{ kN/m}^3$
Peak strength	$c'_p = 7 \text{ kPa}, \phi'_p = 20^\circ$
Residual strength	$c'_r = 2 \text{ kPa}, \phi'_r = 13^\circ$
Nonlocal plastic strain limits	$\epsilon_p^{p*} = 5\%, \epsilon_r^{p*} = 20\%$
Voids ratio	$\mu = 0.2$
Stiffness, Young's Modulus	$E = 25 (p' + 100)$ min 4000kPa
Coefficient of Earth Pressure at rest	$K_0 = 2.0$
Permeability	$k_0 = 5 \times 10^{-10} \text{ m/s}$ $b = 0.003 \text{ m}^2/\text{kN}$
Angle of Dilatation	$\psi = 0^\circ$

2.1 Boundary conditions

Coupled consolidation analyses were performed using the Imperial College Finite Element Program (ICFEP). Plane strain eight-noded isoparametric elements with reduced integration were used. An accelerated modified Newton-Raphson scheme with a sub-stepping stress point algorithm was employed to solve the nonlinear finite element equations (Potts & Zdravkovic 1999). No horizontal displacement was allowed on the vertical boundaries, whereas the bottom boundary was fixed in both horizontal and vertical directions (Figure 1).

Before excavation of the slope, initial stresses are specified in the soil using a bulk unit weight of $\gamma = 18.8 \text{ kN/m}^3$ and a uniform coefficient of lateral earth pressure $K_0 = 2$. The pore water pressures are hydrostatic with 10kPa suction specified at the soil surface, following the average height expected for the phreatic surface in the UK (Vaughan & Walbanke 1973). Seasonal fluctuations are not modeled. The bottom and side boundaries are impermeable. The permeability, k of the soil is modeled as isotropic and linked to the mean effective stress, p' using the non-linear relationship in Equation 1 (Vaughan 1994).

$$k = k_0 e^{-bp'} \quad (1)$$

The slope was excavated in horizontal layers over 0.25 years. This unloads the soil surrounding the excavation and the low permeability of the soil creates negative pore water pressures. After excavation 10kPa suction is applied at the free boundary (Figure 1). Time and consolidation allow these excess pore water pressures to slowly dissipate. The changes in pore water pressures and strain softening behaviour of the stiff clay eventually lead to failure of the

slope. The point of failure is defined as the last increment of the analysis that will converge with a time step of 0.01years. Initially time steps of 1 year are employed and the size of the incremental step is reduced as slope failure is approached.

2.2 Nonlocal strain softening soil model

A nonlocal elasto-plastic constitutive soil model is employed to simulate strain softening soil behaviour. A Mohr-Coloumb failure surface is adopted. The soil strength properties, the angle of shearing resistance, ϕ' and cohesion, c' vary with the nonlocal strain ε^{p*} . Peak and residual values are applied before and after the specified nonlocal plastic strain limits respectively (Table 1), with a linear progression between the limits. The nonlocal strain is employed to reduce the mesh dependency of the strain softening calculations (Summersgill et al. 2014). It regulates the reduction in soil strength by referencing a nonlocal strain, which is calculated by relating the surrounding values of local deviatoric plastic strain $\varepsilon^p(x_n')$ to strain at the calculation point, $\varepsilon^p(x_n')$ using a weighting function, $\omega(x_n')$ (Equations 2, 3 and 4). The weighting function uses the G&S modifications (Galavi & Schweiger 2010).

$$\varepsilon^{p*}(x_n) = \frac{1}{V_\omega} \iiint \omega(x_n') \varepsilon^p(x_n + x_n') dx_1' dx_2' dx_3' \quad (2)$$

$$\omega(x_n') = \frac{\sqrt{(x_n' - x_n)^T (x_n' - x_n)}}{l^2} \exp \left[-\frac{(x_n' - x_n)^T (x_n' - x_n)}{l^2} \right] \quad (3)$$

$$V_\omega = \iiint \omega(x_n') dx_1' dx_2' dx_3' \quad (4)$$

The nonlocal length parameter, l controls the shape of the weighting function. It also affects the softening rate of the soil. A value of $l = 1\text{m}$ was used to create an appropriate softening rate with the strain limits of 5% and 20%. An additional nonlocal parameter, the radius of influence, was used to restrict the area of the reference space for the nonlocal calculations and increase numerical efficiency. The radius of influence was set at 3m. With a nonlocal length parameter of 1m and 3m radius of influence the analyses only required a 30% increase in computational time compared to the equivalent analyses employing a local strain softening method (Summersgill 2015).

2.3 Pile Simulation

The mesh has been designed to allow the placement of vertical piles in 26 different locations between the toe and crest of the slope (Figure 1). The length of the pile can be varied at 1m intervals up to 15 meters. In these analyses the pile is wished in place immediately after excavation of the slope.

The pile is modelled using a single column of beam elements placed between the solid quadrilateral elements. These elements are of zero thickness and model the bending behaviour of the pile using the specified stiffness, density, cross sectional area, A and second moment of inertia, I . The simulated pile diameter is 0.9m with a spacing of 2.7m or three diameters. The calculated A and I were divided by the pile spacing to account for the total quantity of soil that would be supported by a discrete pile in a row. A Young's modulus of 14GPa and a density of 2400kg/m³ were specified. A linear elastic constitutive soil model is employed and the maximum bending moment is monitored to identify potential plastic hinge formation.

3 RESULTS

The slope failure mechanism for each analysis can be identified from the contours of accumulated plastic strain or the incremental displacement vectors for the final increment of the analysis. The improvement in the stability of the slope is indicated by the time to slope failure for each analysis, as well as the change in failure mechanism.

For a slope without any stabilisation piles, failure occurred 40.46 years after excavation was complete. The contours of strain showed the development of two potential slip surfaces initiating below the toe of the slope and extending into and towards the crest of the slope. The shallower slip surface became critical. Inserting stabilisation piles that interact with either of the two slip surfaces changed the failure mechanism and time to slope failure. The two sets of analyses presented investigate the influence of pile position and length.

3.1 Pile Position

A 15m long pile was placed in each of the 26 locations between the toe and crest of the slope in Figure 1. These locations are spaced 1.2m apart. The position of the pile was found to have a large influence on the pile and slope failure mechanism. Five failure mechanisms were identified by the pattern of slope and pile movements. The vectors of incremental displacement for the final increment give an example of each mechanism in Figure 2. The sizes of the arrows are relative to the largest incremental displacement for each analysis, but not proportional between the analyses due to the large difference in the size of displacements depending on the mechanism.

The positions of the five analyses shown in Figure 2 are identified in Figure 1 by the thicker coloured lines. The numbers in Figure 1 identify the last pile position for each mechanism type. This is reinforced by the different colours of the bars in Figure 3, comparing the variation in time to failure due to the position of the pile.

Two of the mechanisms, (a) and (e), did not interact with the pile. With a pile at the very toe of the slope, failure occurred above the pile and the time to failure was 3 years less than without a pile. This is likely due to the suppressed movements at the base of the excavation that created non-critical slip surfaces in the no-pile analysis.

The failure of the slope downslope of the pile without pile interaction, mechanism (e), provides a small increase in time to failure of 5 to 23 years. The pile effectively reduces the height of the slope by up to 2.4m, but sufficient height remains for failure of the slope to occur without the contribution of the mass behind the pile to increase the destabilising force. There was therefore very little displacement or bending of the piles in these analyses.

For mechanism (d) the piles did undergo bending and displacement, as it can be seen by the horizontal arrows at the location of the pile and small movements of the soil upslope, Figure 1(d). This resulted in an increase in the time to failure from 40 years to between 57 and 98 years after excavation. This is still likely to be an inadequate improvement in stability for the required lifetime of transport slopes.

Two mechanisms (b) and (c) do provide a significant improvement in time to failure, with ranges of 203 to 224 and 120 to 163 years respectively prior to slope failure. The movement of the pile in these analyses is an integral part of the failure mechanism. The pile movement occurs due to the force from the soil upslope or the movement of soil downslope reducing support in front of the pile.

In mechanism (c), it is a combination of these two movements causing upslope and downslope failure. Slip surfaces

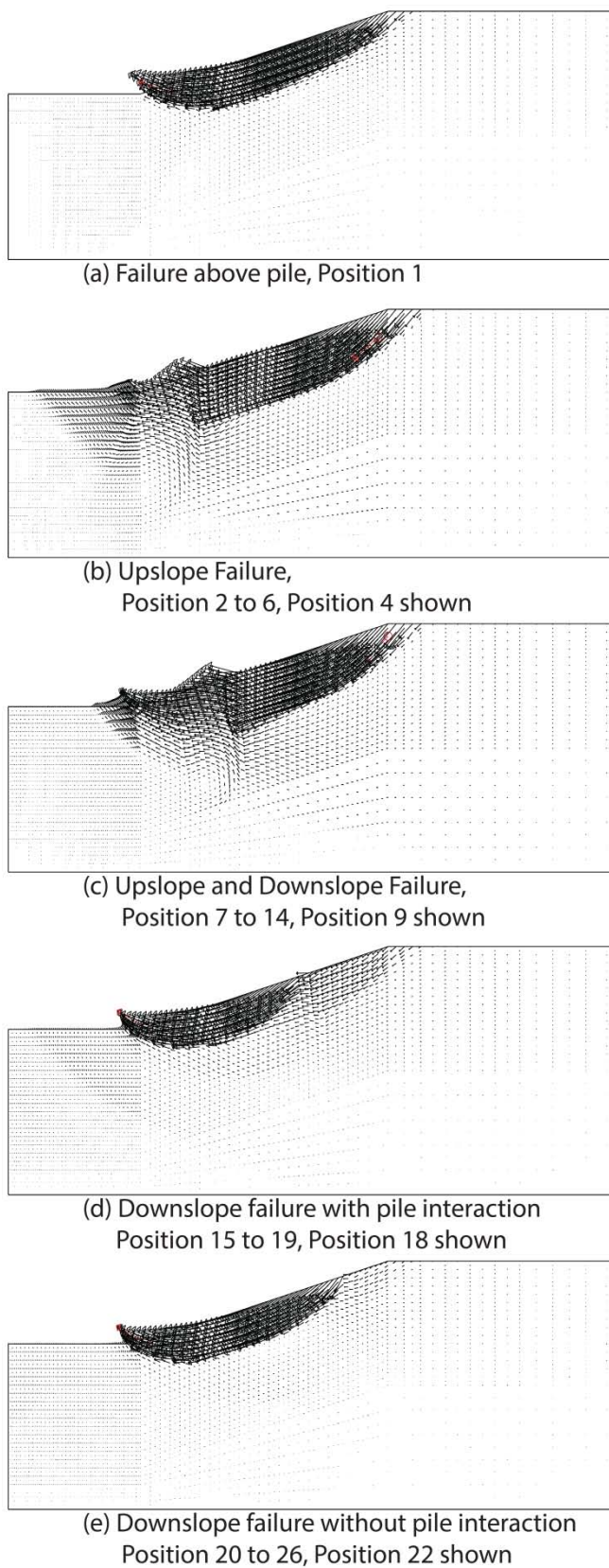


Figure 2. Pile and slope failure mechanisms, shown by the incremental displacement vectors for the final increment of an analysis.

have formed downslope of the pile in the same area as the no-pile analysis, Figure 4(a). Movement on these slip surfaces contributes to slope movement and is the reason for a smaller time to failure than mechanism (b). In mechanism (b), sufficient soil is present behind these locations to move the pile downslope and form a slip surface upslope. The soil downslope in mechanism (b) positions is pushed into the excavation, but has not formed its own slip surface.

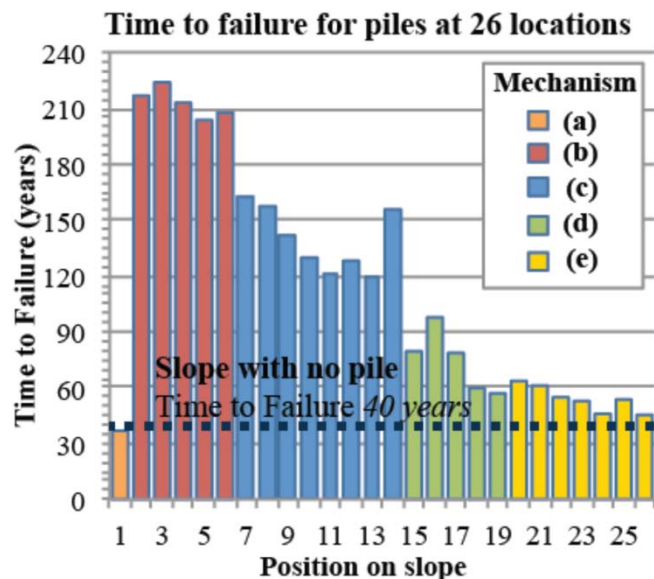


Figure 3. Comparison of time to failure depending on the position of the pile between the toe and crest of the excavated slope.

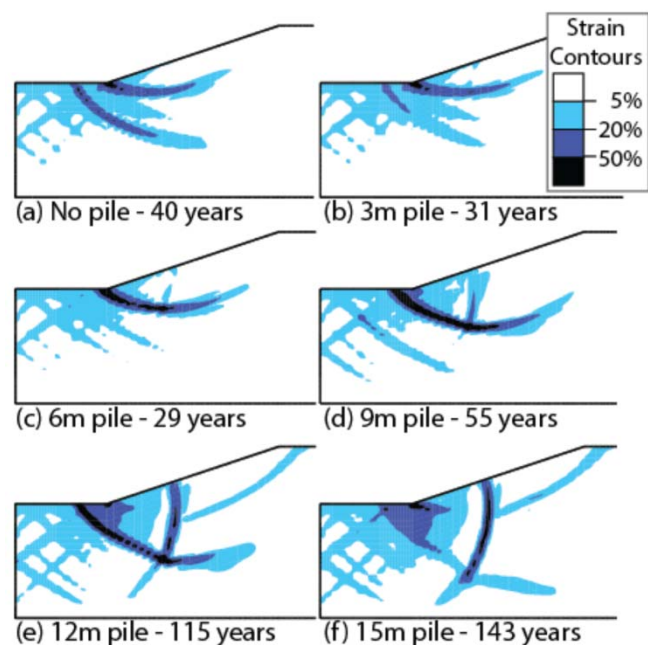


Figure 4. Accumulated plastic strain contours for the last increment of the analysis, showing the influence of pile length on mechanism and time to failure.

The presence of the pile does not prevent soil movement, which occurs as a reaction to slope excavation and high lateral soil stresses. The pile is most effective when it interacts with the development of the slip surface and affects the failure mechanism. For these slope dimensions, this occurs in the bottom half of the slope, but not at the very toe of the slope. The piles placed in the top half of the slope create only marginal improvements.

3.2 Pile Length

The variation of pile length had a significant influence on the stabilizing effect of the pile. The analyses for a pile in position 9 with different lengths are presented in this section. The analysis for the 15m length pile is the same analysis as shown in Figure 2(c). Additional analyses varying the pile length from 3m to 12m at 3m intervals are presented with the 15m results in Figure 4. The accumulated strain contours show the position and relative development of slip

surfaces, both critical and non-critical. The change in strain development for these analyses is directly compared to the analysis without a pile, Figure 4(a).

The time to failure for each analysis is stated on the label. Constructing a pile 3m or 6m in length immediately after excavation reduced the stability of the slope by a quarter compared to not constructing a pile. A 3m pile does not intersect the shallow slip surface and a 6m pile barely intersects this surface. The critical slip surface forms beneath the base of the pile, translating it within the unstable mass. Furthermore, the presence of the pile encourages the development of the critical surface, reducing the time to slope failure and development of other slip surfaces.

The 9m pile provides some improvement by increasing the depth of the critical slip surface, but it can still pass beneath the pile (Figure 4(d)). With a 12m pile, a mechanically viable slip surface cannot form underneath the pile. The slip surface formed down-slope of the pile and pressure from the soil behind the pile eventually causes sufficient bending of the pile for a slip surface to form upslope. This requires a longer period for development, extending the stability of the slope to 115 years. The further increase in pile length to 15m requires even more time. This is likely due to the reduced movements downslope of the pile because the base of the 15m pile is too deep to interact with soil movement at the toe of the slope in the same way as the 12m pile.

The behaviour with pile length discussed here is only valid for position 9 in the slope with less than 10m of soil below the base of the pile. It would be expected for the impact of pile length to vary with location and depth to bedrock, reflecting the changing interaction of the pile and mechanically viable slip surfaces.

4 CONCLUSION

The interaction of a vertical stabilisation pile and slope is complex. Construction of a pile does not provide a single stabilising action at the intersection with the critical slip surface of the unstabilised slope. Moreover, the pile is most effective in extending the stability of the slope when the failure mechanism is significantly altered by the presence of the pile. An oversimplification during design could miss the critical failure mechanism or provide a conservative stabilisation solution.

The pile position and length have a large influence on the stabilising effect of the pile. The pile should be designed to interact with all potentially critical slip surfaces. These analyses demonstrated that for stiff clay excavated slopes the pile should be placed between the midslope and the toe of the slope, although not exactly at the toe of the slope. For the presented example of a 10m high, 1 in 3 angled slope, a pile placed one third in from the toe of the slope should be more than 9m long to provide a reasonable improvement in stability.

These analyses indicate the sensitivity of the discrete pile row and slope interaction to pile design. In addition to pile length and position, further factors to consider would include the pile diameter, spacing, stiffness, time of pile construction and 3D analyses modelling arching between piles. Without an understanding of these factors, a simplified design method could provide misleading results.

ACKNOWLEDGEMENT

This research was funded by the UK's Engineering and Physical Sciences Research Council (EPSRC) and Geotechnical Consulting Group Llp.

REFERENCES

Baguelin, R. Frank, R. & Said, Y.H. 1977. Theoretical study of lateral reaction mechanism of piles, *Geotechnique* **27:3**,

405–434.

Carder, D. 2009. *Improving the stability of roads using a spaced piling technique*, TRL Report, United Kingdom.

Ellis, E.A. Durrani, I.K. & Reddish, D.J. 2010. Numerical modelling of discrete pile rows for slope stability and generic guidance for design, *Geotechnique* **60:3**, 185–195.

Ellis, E.A. & O'Brien, A.S. 2007. Effect of height on delayed collapse of cuttings in stiff clay, *Proceedings of Institution of Civil Engineers: Geotechnical Engineering* **160:2**, 73–84

Galavi, V. & Schweiger, H.F. 2010. Nonlocal multilaminate model for strain softening analysis, *International Journal of Geomechanics* **10**, 30–44.

Hassiotis, S. Chameau, J.L. & Gunaratne, M. 1997. Design method for stabilisation of slopes with piles, *Journal of Geotechnical and Geoenvironmental Engineering* **123:4**, 314–323.

Potts, D.M. Kovacevic, N. & Vaughan, P.R. 1997. Delayed collapse of cut slopes in stiff clay, *Geotechnique* **47:5**, 953–982.

Potts, D.M. & Zdravkovic, L. 1999. *Finite Element analysis in geotechnical engineering: Theory*, Thomas Telford, London.

Summersgill, F.C. Kontoe, S.K. & Potts, D.M. 2014. A comparison of the mesh dependence of the local and nonlocal strain softening methods in a biaxial compression analysis. *Numerical methods in geotechnical engineering: Proceedings, 8th NUMGE* (Eds: Hicks, M.A. Brinkgreve, R.B.J. & Rohe, A.), 289–294. Taylor & Francis, London.

Summersgill, F.C. 2015. *Numerical modeling of stiff clay cut slopes with nonlocal strain regularisation*. PhD Thesis, under preparation, Imperial College London.

Wilkinson, S. Brosse, A. Fenton, C. Hosseini Kamal, R. Jardine, R.J. & Coop, M.R. 2011. An integrated geotechnical study of UK mudrocks. *Geotechnics of Hard Soil – Weak Rocks: Proceedings, 15th ECSMGE* (Eds: Anagnostopoulos, A. Pachakis, M. & Tsatsanifos, C.), 305–310. IOS Press, Amsterdam.

Vaughan, P.R. & Walbancke, H.J. 1973. Pore pressure changes and the delayed failure of cutting slopes in over-consolidated clay, *Geotechnique* **23:4**, 531–539

Vaughan, P.R. 1994. Assumption, prediction and reality in geotechnical engineering, *Geotechnique* **44:4**, 573–603

Numerical modelling of wave attenuation through soil

Modélisation numérique de la propagation dans le sol des vibrations

R. Colombero, S. Kontoe, S. Foti and D. M. Potts

ABSTRACT Numerical analyses of induced ground vibrations play an important role in assessing building safety and comfort. One of the major difficulties is related to the calibration of an adequate source model to be used in the numerical simulation. In this paper the attenuation of waves caused by drop load tests is considered to provide a general framework for the evaluation of vibration attenuation both with empirical laws and numerical simulations. A new equation to reproduce the source signal is suggested and used as input for a dynamic coupled consolidation Finite Element Analysis. The model is validated through comparison with field data obtained at a site in the vicinity of the Tower of Pisa, Italy, from geophones at various distances from the impact source. The calibrated numerical model is then used to study in detail the attenuation of waves from the source and assess the validity of empirical attenuation laws.

1 INTRODUCTION

Surface wave tests, including drop load tests, are often used for site characterisation (Foti et al. 2014). These tests are non-intrusive and can be used to obtain shear wave velocity and material damping profiles at a site.

Several analytical expressions have been developed in the past to reproduce the source pulse generated by drop load tests (Pekeris 1955; Mooney 1974; Abe et al. 1990). However, only a few of these provide a good match to real data. As the influence of the drop load apparatus set-up is found dominant on the resultant wave field, a new expression for the disturbing source signal is proposed, based on experimentally recorded signals, generated by a well characterised source.

Several factors contribute to the attenuation of the vibration amplitude with the distance in the ground. The most important contributions are given by geometrical wave spreading, material damping and scattering due to heterogeneities in the soil: the first component following a power law with the distance from the source, the latter two an exponential law (Auersch 2010).

Numerical simulations of the case study of Pisa, Italy, were carried out to validate wave velocity distance attenuation relationships. The layered soil profile was modelled in detail in the finite element model and the input drop load action was based on a novel expression for the disturbing source pulse. The numerical model was considered to be reliable in reproducing the attenuation of the wave generated by drop load tests, as a very good agreement between the experimental and the computed peak particle velocity (PPV) decay trends with distance was achieved.

2 AMPLITUDE-DISTANCE ATTENUATION LAWS

2.1 Theoretical framework

2.1 Theoretical framework

Any disturbing source, as simple as an impulse, acting on a medium generates a complex wave field. The amplitude of such waves decays with distance as the waves propagate away from the source. The main mechanisms that influence the attenuation of impact induced vibrations (Semblat & Pecker 2009; Auersch 2010) are:

- Geometrical attenuation: based on the elastic wave energy conservation, the amplitude A of waves generated at a point attenuate with distance r following a power

law $A \propto r^{-n}$, where A represents the wave velocity amplitude and r is the distance from the source position. The exponent n takes values of 0.5 or 2.0 respectively for surface and body waves produced by a surface point load (Auersch 2010).

- Material attenuation and scattering in nonhomogeneous media: the hysteretic behaviour of the soil and the wave refraction at interfaces between layers lead to a second attenuation component, exponentially dependent on the distance, $A \propto \exp(-k.r)$, where the coefficient k accounts for material damping, soil natural frequency and surface wave characteristics (Auersch 2010).

2.2 Amplitude-distance attenuation laws for waves induced by impact loads

It has been argued that the exponential term has only a minor influence on the energy reduction of ground vibrations induced by impact sources as the distance increases (Auersch & Said 2010). Hence it can be neglected and the attenuation of the vibrations can be approximated by a power law of similar form to the theoretical one: $A \propto r^{-q}$. Various experimental velocity recordings have been analysed to assess the attenuation of impact-induced vibrations and the exponent q was found to change according to the type of source and type of soil profile (Auersch & Said 2010). The experimental exponent q has been found varying between values of 1.0 and 1.6 for drop load tests carried out on sandy and clayey soils respectively (Auersch 2010).

Further experimental studies (Mooney 1976) correlate the vibration amplitude A of the induced wavefield with the distance r from the disturbing source through a power law and with the characteristics of the source as defined below:

$$A = C \cdot H_s \cdot r^{-n} \cdot T_s^{-m-p} \quad (1)$$

Where H_s and T_s are the source pulse and period respectively; C is a constant; $m+p=1.4$ and $n=0.5$ are the surface wave velocity exponents.

Equation (1) can be expanded taking into account also the effect given by the exponential term to obtain a complete attenuation law that can be applied to drop load tests:

$$A = C \cdot H_s \cdot R^{-n} \cdot T_s^{-m-p} \cdot \exp(-kR) \quad (2)$$

Where $k=2n\xi$ (with ξ material damping); n is the effective surface wave velocity attenuation exponent; and $R = r / \lambda_R$, with λ_R the surface waves wavelength.

3 DROP LOAD TESTS AND ANALYTICAL REPRESENTATION OF DISTURBING SOURCES

Drop load tests consist of a falling heavy weight hitting a plate or directly the ground, generating a wave field. Particle velocity signals are captured at different distances from the source by geophones (Foti 2000; Figure 1).

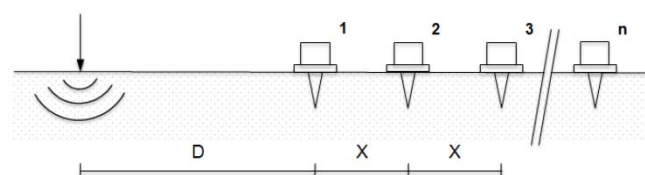


Figure 1. Experimental setup for multistation SASW tests

Early attempts to evaluate the soil response due to a surface point force were based on the disturbing action represented by a vertical impulse (Lamb 1904; Mooney 1974), a step unit function (Pekeris 1955) or sinusoidal functions (Mooney 1974; Abe et al. 1990).

In the latest studies the amplitude of the source signal was found proportional to the momentum of the weight before the impact (given by the product of mass by velocity just before the impact).

From the analysis of near-field observations of particle velocity time histories recorded by geophones, a new more accurate expression is derived. A Gabor wavelet (Semblat & Pecker 2009) formed the basis of the new function, then modified to account for the momentum of the dropped weight C_b in order to approximate the pulse produced by a mass falling on the ground (Figure 2, equation (3)).

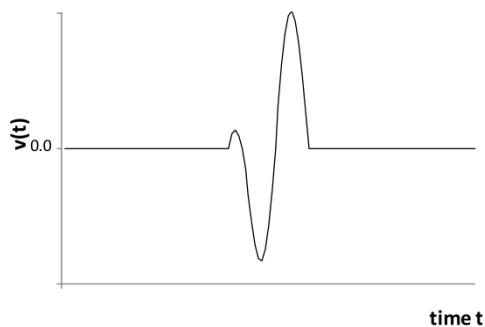


Figure 2. Modified Gabor wavelet

$$v(t) = \begin{cases} C_b \cdot \beta \cdot t^\gamma \cdot \exp\left[-\left(\frac{2\pi}{T_s \alpha} t\right)^2\right] \cos\left(\frac{2\pi}{T_s} t\right), & 0 \leq t \leq 1.2T_s \\ 0, & \text{otherwise} \end{cases}$$

where t is a generic time instant; T_s the period of the function; and α , β , and γ are constants.

4 SITE DESCRIPTION AND FIELD DATA

The subsoil of Piazza dei Miracoli, Pisa (Italy) has been extensively characterised in the last decades as the basis for the stabilisation design of the Tower.

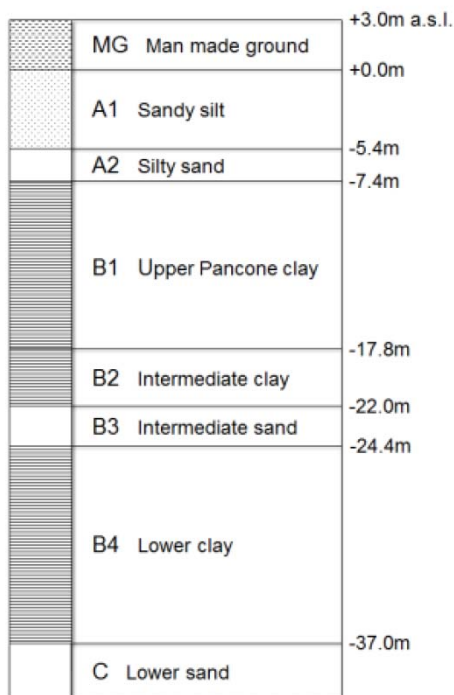


Figure 3. Indicative stratigraphy retrieved in Piazza dei Miracoli, Pisa

The soil stratigraphy beneath Piazza dei Miracoli presents a sequence of sand and clay formations and is represented in

Figure 3. Seismic Analysis of Surface Waves tests (SASW), including drop load tests, were performed in Piazza dei Miracoli next to the Tower (Foti 2003).

The drop load test configuration consisted of a 130 kg weight dropped from a height of approximately 3 m, hitting the ground directly in order to avoid mass rebound and to reach lower frequencies. The vibrations at the surface were recorded by 24 in-line geophones at 2.5m spacing.

Figure 4 shows the velocity time histories recorded at 5, 35 and 60m from the source location. The increase in the significant duration of the motion with distance is due to increasing shear wave velocity with depth, i.e. the dispersive behaviour of the soil, typical of heterogeneous media.

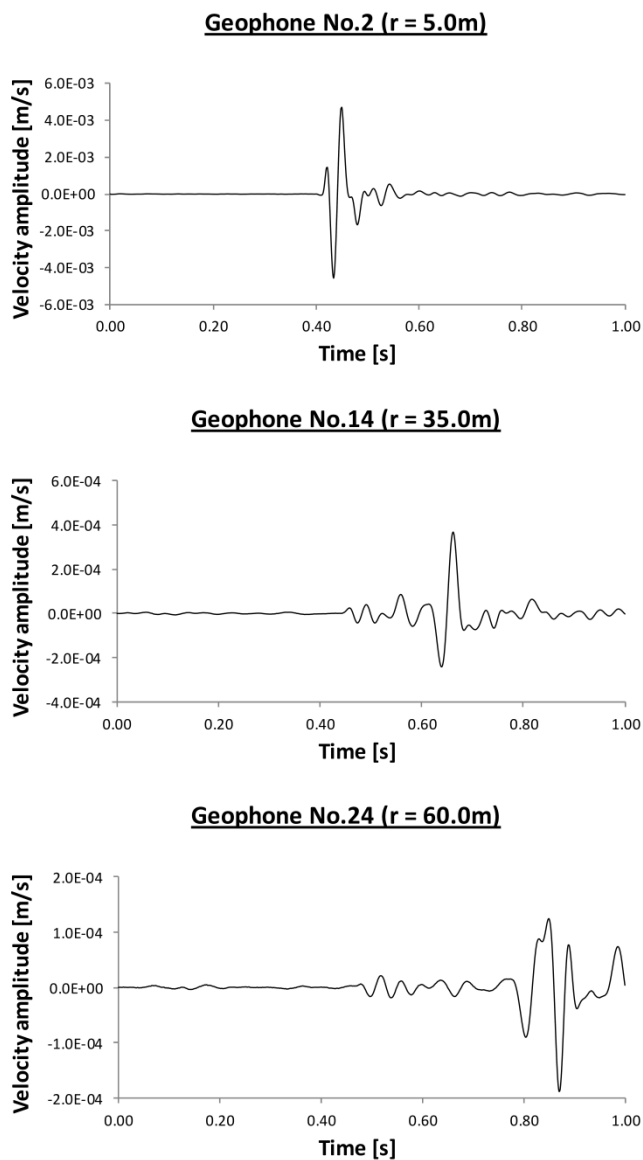


Figure 4. Velocity time histories recorded at $r = 5, 35$ and 60 m from the source

5 NUMERICAL MODEL DESCRIPTION

Fully coupled finite element simulations of the droplload tests carried out in Pisa were performed in the time domain with the code ICFEP (Potts & Zdravkovic 2001). The precise evaluation of the model input parameters is of primary importance for the accurate representation of the impact-induced wavefield.

The domain discretisation for the simulation of the drop load tests consisted of: two-dimensional axisymmetric configura-

tion; mesh dimensions 160m x 53m; total number of 9472 eight-noded quadrilateral solid elements to define the mesh; horizontal displacements restricted along the left lateral boundary to account for symmetry of the problem; tangential and normal to boundary dashpots applied at the bottom and right lateral boundaries to absorb wave reflections; zero pore pressure at water table depth (assumed 1.3m bgl); and disturbing action applied at the top left node of the model.

As the impact source used in the tests performed in Pisa was not monitored, the modified formulation of the Gabor wavelet (Semblat & Pecker 2009, equation (3)) was considered as the model synthetic input source signal, employing the following parameters: $a = 7$; $\beta = 1.55 \cdot 10^{-2}$; $\gamma = 1.2$; $T_s = 0.04s$; and $C_b = 997.4 \text{ kg.m/s}$. These parameters were obtained with a calibration on the signal at the first geophone.

The properties assigned to the materials are shown in Table 1. The material damping of the soil profile was approximated with the Rayleigh damping formulation, based on a target damping ratio varying with depth (Foti 2003). Incomplete saturation of nearsurface layers was also approximated in the analyses (Table 2) by appropriately reducing the corresponding pore fluid compressibility.

Table 1. Soil properties used in the finite element analysis – V_s : shear wave velocity; γ : bulk unit weight; E : soil stiffness; ν : Poisson's Ratio; ξ^* : target damping ratio; K : permeability

Layer	V_s [m/s]	γ [kN/m ³]	E [MPa]	ν []	ξ^* [%]	K [m/s]
MG	155	19.00	124	0.33	7.0	1E-07
A1	180	18.50	163	0.33	5.4	1E-07
A2	170	18.00	141	0.33	2.5	5E-07
BI	150	16.75	102	0.33	3.1	9E-09
BII	235	19.50	2920	0.33	2.0	8E-09
BIII	245	18.75	3051	0.33	2.0	5E-07
BIV	215	18.00	226	0.33	2.0	8E-09
C	380	20.00	783	0.33	2.0	5E-7

Table 2. Partial saturation characteristics - K_f : bulk modulus of fluid and S_r : correspondent saturation

Layer	K_f [kPa]	S_r [%]
Layer MG (above water table)	9954.8	99.00%
Layer MG (below water table)	19819.8	99.50%
Layer A1 ($V_p < 1400 \text{ m/s}$, 6m bgl)	592710.5	99.981%
Layer A1 ($V_p > 1400 \text{ m/s}$)	2.2E6	100.00%
Layers A2 ÷ C	2.2E6	100.00%

6 RESULTS

The results from the finite element simulation have been compared with the field measurements. To get a representative response for near-field, far-field and intermediate conditions, geophones at 5m, 35m and 60m distance from the disturbing source are reported.

6.1 Comparison with the field data

The experimental recordings at the geophones are com-

pared to the numerical results in Figure 5.

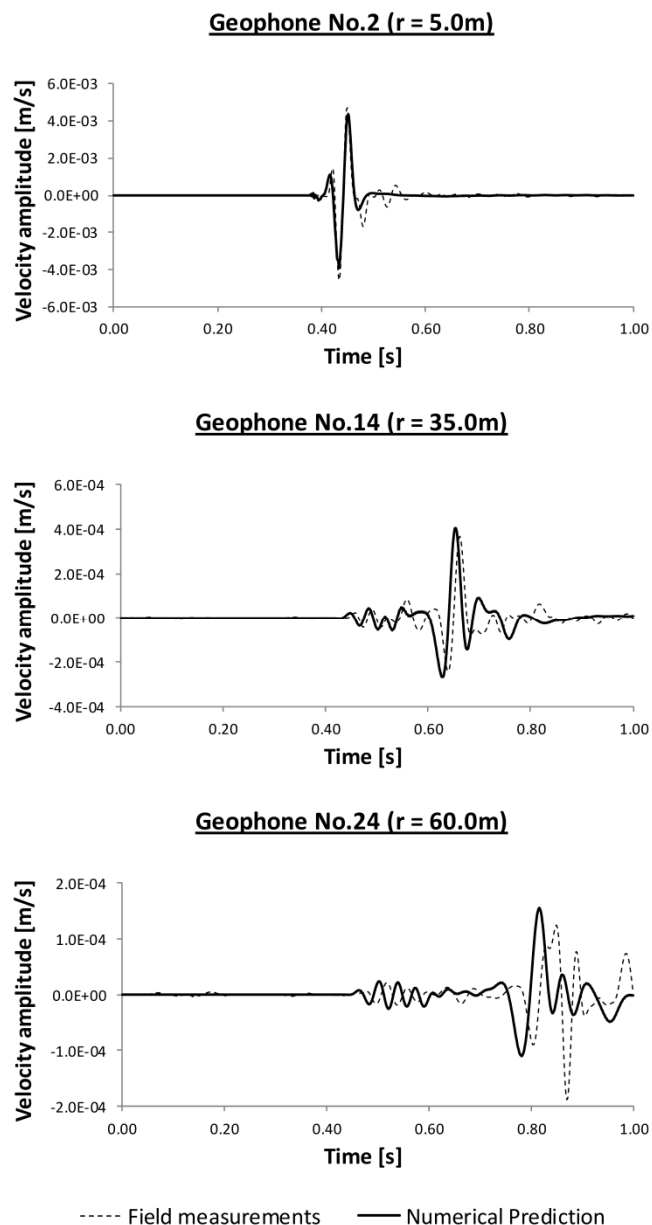


Figure 5. Comparison of the experimental and numerical time histories (at $r = 5, 35$ and 60 m from the source)

High resemblance is achieved between the signals, in particular in the near- and middle-field, while in the far-field a faster wavefield propagation in the soil is predicted. The waves of smaller amplitude (registered after the major tremor) due to wave reflections and refractions in the soil deposit are not well captured by the numerical model. These inaccuracies in the response are mainly due to the simplifications used in the numerical model, e.g. uncertainties in the degree of soil saturation and the use of a synthetic source signal based on a single central frequency (25 Hz).

6.2 Comparison of the PPV trend with literature equations

The most effective approach to analyse the attenuation of ground vibrations is the analysis of the peak particle velocities (PPVs) recorded by each geophone. The magnitude of the peak particle velocities recorded in Pisa decreases from 9 mm/s at a distance of 2.5 m from the source to 0.2 mm/s at a distance of 60 m (Figure 6, white circles).

The previously mentioned analytical and empirical attenuation equations are presented for comparison. In Figure 6 both experimental data and numerical predictions are ap-

proximated by the power law $A \propto r^{-q}$, which gives a straight line on a double logarithmic plane with slope $q = 1.282$ and $q = 1.272$ respectively. An accurate modelling has therefore been achieved and this power attenuation law is found to be able to reproduce the wave amplitude decay with sufficient accuracy for preliminary design purposes. A second comparison is made against the complete attenuation law given by equation (2) for both experimental and numerical data (Figure 7 and Figure 8 respectively). The input coefficients are $T_s = 0.04s$; $H_s = 0.145$ mm/s; $k = 0.302$; $C = 3800$; $m+p = 1.4$; and $n = 075$.

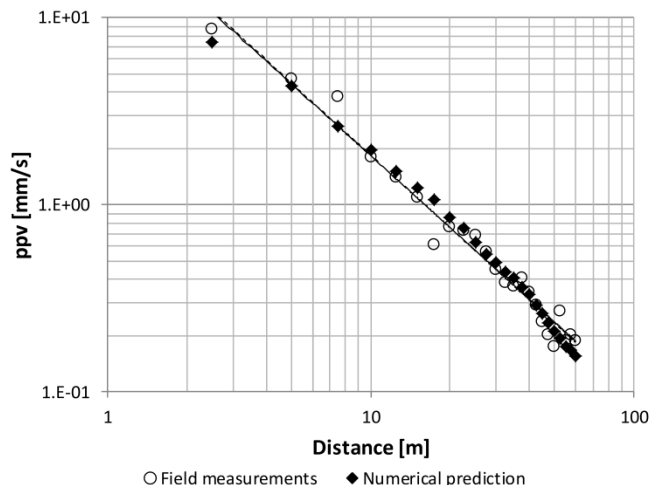


Figure 6. Comparison of the experimental and numerical PPV attenuation curves

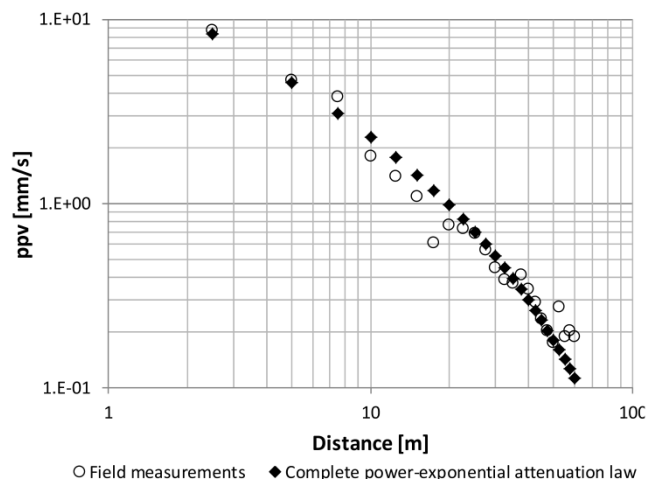


Figure 7. Comparison of the field measurements attenuation curve with the amplitude-distance curve given by equation (2)

The very good agreement between the complete law and the measured attenuation trend demonstrates the importance of the exponential component, related to the soil material, to the overall attenuation.

7 CONCLUSIONS

This study investigated the attenuation of ground vibrations generated by drop load tests and compared analytical and empirical expressions with the attenuation predicted by numerical analysis using as a reference the field data from the well-documented case study of Pisa.

The soil response due to a weight falling on the ground has been investigated in previous studies. The simplified source signal and homogeneous soil representation previously proposed were revised to obtain a better representation of the disturbing action produced by drop load tests. A new ex-

pression (equation (3)) is presented which for the examined case study was shown to successfully represent the impact source, but further analysis is needed to confirm its applicability.

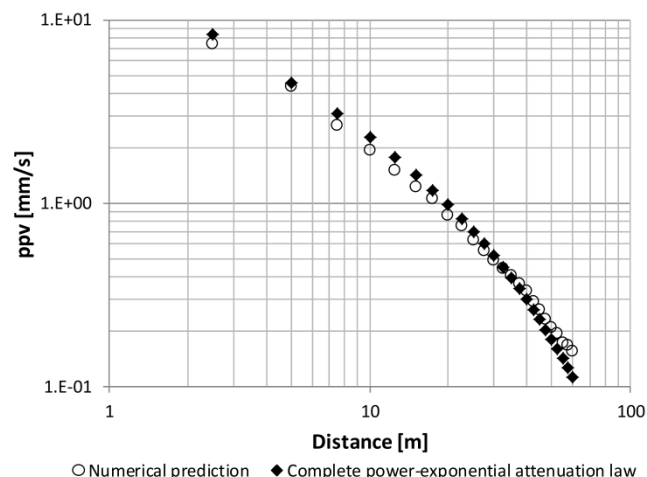


Figure 8. Comparison of the numerical PPV attenuation curve with the amplitude-distance curve given by equation (2)

Two main factors contribute to the attenuation of impact-induced waves in the ground: geometrical spreading and material damping, following a power and exponential attenuation law respectively. Numerous equations have been suggested in previous studies to reproduce the decay of the waves with distance. A simplified power law and a complete power exponential law were examined in this study. Both expressions exhibited good agreement with the field data of drop load tests carried out in Pisa, but the superiority of the complete law was evident.

As an independent assessment of the existing analytical attenuation expressions, a numerical simulation of the drop load tests was performed with the finite element program *ICFEP* (Potts and Zdravkovic 2001). The agreement of the numerical results with the experimental recordings shows how an excellent prediction of the induced ground vibrations can be achieved on the basis of a good site characterisation and a monitoring device close to the source.

REFERENCES

- Abe, S. Kobayashi, Y. & Ikawa, T. 1990. Seismic characteristics of the weight-dropping source. *Journal of Physics of the Earth* **38** (3), 189-212.
- Auersch, L. 2010. Technically Induced Surface Wave Fields, Part I: Measured Attenuation and Theoretical Amplitude-Distance Laws. *Bulletin of the Seismological Society of America* **100** (4), 1528-1539.
- Auersch, L. & Said, S. 2010. Attenuation of ground vibrations due to different technical sources. *Earthquake Engineering and Engineering Vibration* **9** (3), 337-344.
- Foti, S. 2003. Small-strain stiffness and damping ratio of Pisa clay from surface wave tests. *Geotechnique* **53** (5), 455-461.
- Foti, S. 2000. Multistation methods for geotechnical characterization using surface waves. *PhD Degree in Geotechnical Engineering, Department of Structural and Geotechnical Engineering*. Technical University of Turin (Politecnico), Italy.
- Foti S. Lai C.G. Rix G.J. & Strobbia C. 2014. *Surface Wave Methods for Near-Surface Site Characterization*. CRC Press, Boca Raton, Florida (USA).

Lamb, H. 1904. On the propagation of tremors over the surface of an elastic solid. *Philosophical Transactions of the Royal Society of London. Series A, Containing papers of a mathematical or physical character* **203**, 1-42.

Mooney, H. M. 1976. The seismic wave system from a surface impact. *Geophysics* **41** (2), 243-265.

Mooney, H. M. 1974. Some numerical solutions for Lamb's problem. *Bulletin of the Seismological Society of America* **64** (2), 473-491.

Pekeris, C. 1955. The seismic surface pulse. *Proceedings of the National Academy of Sciences of the United States of America* **41** (7), 469.

Potts, D.M. & Zdravković, L. 2001. *Finite element analysis in geotechnical engineering: theory*. Thomas Telford, London.

Semblat, J.J. & Pecker, A. 2009. *Waves and vibrations in soils*. Iuss Press, Pavia.

Technical Note: CCR Closure and Geocomposite Drainage



This technical note focuses on CCR closure and post-closure care for facilities closing with the coal combustion residual waste remaining in place. In the United States, the Resource Conservation and Recovery Act (RCRA) placed the authority and the responsibility on the [US Environmental Protection Agency](#) (EPA) to establish rules and regulations for solid waste disposal management practices "to ensure no reasonable probability of adverse effects on human health or the environment from the disposal of solid wastes." After years of assessing the management practices associated with the storage and disposal of a particular solid waste, coal combustion residual materials (CCR), EPA established in April of 2015 nationally applicable minimum criteria for CCR landfills and CCR surface impoundments to be constructed and to operate as sanitary disposal facilities under RCRA. These minimum criteria are documented in the Code of Federal Regulations Title 40 Parts 257.50 through 257.107 (the Code). The criteria may be grouped into seven sets of criteria, restrictions and/or requirements the owners and operators of CCR facilities must comply with to establish new facilities, continue to operate existing facilities, and close and care for facilities at the end of their useful lives.

The seven criteria:

- Location restrictions
- Liner design criteria
- Structural integrity requirements
- Operating Criteria
- Groundwater monitoring and corrective action requirements
- Closure and post-closure care requirements
- Recordkeeping, notification and internet posting requirements

Here, the federal standards apply directly to the owners and operators of CCR facilities; they are self-implementing.

Since October 2015, facility owners and operators have been directly responsible for compliance to these standards.

CCR CLOSURE AND POST-CLOSURE CARE REQUIREMENTS

The Code sets out minimum standards for the design, execution and operation of the cover system. The minimum standards are based upon practices found to contribute to the long term performance of the closed facility. Owners and operators must ensure that closure systems for such CCR facilities will, at a minimum, comply with the performance standards identified at 257.102(d)(1) in the Code:

- Control, minimize or eliminate, to the maximum extent feasible, post-closure infiltration of liquids into the waste and releases of CCR, leachate, or contaminated run-off to the ground or surface waters or to the atmosphere
- Preclude the probability of future impoundment of water, sediment, or slurry
- Include measures that provide for major slope stability to prevent the sloughing or movement of the final cover system during the closure and post closure care period
- Minimize the need for further maintenance of the CCR unit; and
- Be completed in the shortest amount of time consistent with recognized and generally accepted good engineering practices.

In the preamble, EPA further stated a number of positions they adopted for rulemaking as a result of their findings.

- The risks to human health and the environment are primarily driven by older units many of which are unlined.
- The final rule does not require the use of composite final covers, such as a geomembrane underlain by a compacted soil infiltration layer. ... Nonetheless, in certain locations, composite cover systems may be necessary to achieve the rule's performance standards.
- Fewer problems are typically seen with the use of composite cover systems. And while ongoing oversight and proper maintenance is necessary to ensure the efficacy of any cover system, less effort is generally involved to ensure the continued performance of a composite cover system. EPA therefore generally recommends that facilities install a composite cover system, rather than a compacted clay barrier, as the composite system has often proven to be more effective (and cost effective) over the long term. For these reasons, EPA also anticipates that composite cover systems will be recommended in many circumstances by qualified Professional Engineers.
- Under the established performance standard, if the cover system results in liquids infiltration or releases of leachate from the CCR unit, the final cover would not be an appropriate cover. Owners and engineers must ensure that in designing a final cover for a CCR unit they account for any condition that may cause the final cover system not to perform as designed. The final rule requires the final over system design to be certified by a qualified professional engineer that the design meets both the performance standard and cover system criteria.

DESIGN OBJECTIVES: GEOCOMPOSITE DRAINAGE

Geocomposite drainage materials have been extensively and successfully used in solid waste landfill closures for decades. The same engineering design methodologies can apply to CCR final cover systems for the long-term compliance of the above referenced performance standards.

Drainage geosynthetics are composed of a geonet core with a geotextile laminated to one or both sides. A geocomposite drain is designed for in-plane flow over a large surface area. The critical engineering properties of a geocomposite drain include its flow capacity (or transmissivity) under design loads and boundary conditions. The flow capacity of a geocomposite is evaluated using a laboratory transmissivity test (ASTM D-4716). This equipment allows a range of normal loads and boundary conditions, i.e., soil vs. rigid membrane, to be applied to the face of the geocomposite. The head acting across the 12-inch square sample can be varied to create a range of gradients that simulate field slope conditions. Be aware that the transmissivity of a geonet core is not representative of the geocomposite, even though it is made of the same geonet core. If the end product is a geocomposite, transmissivity test data must therefore be obtained from a geocomposite. The geotextile portion of the geocomposite functions as a filter and separator, therefore, the geotextile should meet filtration and retention criteria, and it is specific to the on-site soil. The interface shear strength of the geocomposite against adjacent soils and/or other 'geo' layers can be verified using the direct shear test (ASTM D5321).

To satisfy the performance standards for a CCR closure, the engineering design must demonstrate slope stability and among other performance standards minimize to the maximum extent feasible post-closure infiltration of liquid into the waste. The presence of a barrier layer within the final cover invites sliding failure of the cover soil on side slopes due to a buildup of pore water pressures above the barrier layer. To ensure the side slope stability of a final cover, proper design of a drain layer over the liner is essential.

The designer must confirm that (1) the interface friction between any two layers of the cover is adequate, (2) the capacity to drain water infiltrating the cover soil is sufficient to eliminate seepage forces detrimental to slope stability. For project design scenarios with flatter grades (2 to 8%), slope stability is not a major concern, therefore eliminating infiltration becomes the primary design objective. Minimizing the head acting on the barrier layer controls infiltration of liquid through holes in the liner.

Design Rate of Fluid Supply

The greatest uncertainty in the design of the geocomposite drain is accurately predicting the maximum rate of water infiltration. This rate is dependent upon both future extreme weather events and the materials placed over the drain. One of the common methods used to evaluate both the design rate of fluid supply and lateral drainage system performance is EPA's HELP model. This water-balance model allows the designer to evaluate the performance of a given barrier exposed to synthetic or historical weather data. Unfortunately the HELP model does not provide a conservative design for lateral drainage systems. Soong and Koerner (1997) studied eight seepage induced landfill slope failures and found that the HELP model under predicted the required hydraulic capacity of the lateral drains by factors ranging from 10 to 100! Their work suggests that the 24-hour time step employed by HELP and failure to correctly anticipate extreme weather events are the major sources of error. The extreme weather generated by 'El Nino' has made this prediction easier. The high precipitation and mild weather that has accompanied 'El Nino' can produce saturated conditions in the vegetative layer.

The design of the pore water pressure drain underlying a saturated vegetative layer was first presented by Thiel and Stewart (1993). The rate of water infiltration into the geocomposite drain can be readily determined since the water is moving down under a unit gradient such that the infiltration velocity is equal to the permeability of the vegetative layer. Typical permeabilities for such systems range from 5×10^{-3} to 5×10^{-4} cm/sec. Tighter soils do not allow

root penetration and soils looser do not provide adequate water storage (Richardson and Zhao, 1998).

Design Equations for Geocomposite Drainage

Using Darcy's Law, the flow velocity within a cover soil under a unit gradient is equal to the permeability of the material. This represents a design limit and is fortunately more definable than future extreme storm events. Water balance in a closure system is shown in Figure 1. The quantity of water, Q_{in} , infiltrating into a unit width of drainage composite having a length L is given by

$$Q_{in} = k_{veg} \times L \times i \quad (1)$$

Where k_{veg} is the permeability of the vegetative supporting layer of the cover, and L is the drainage length, measured horizontally.

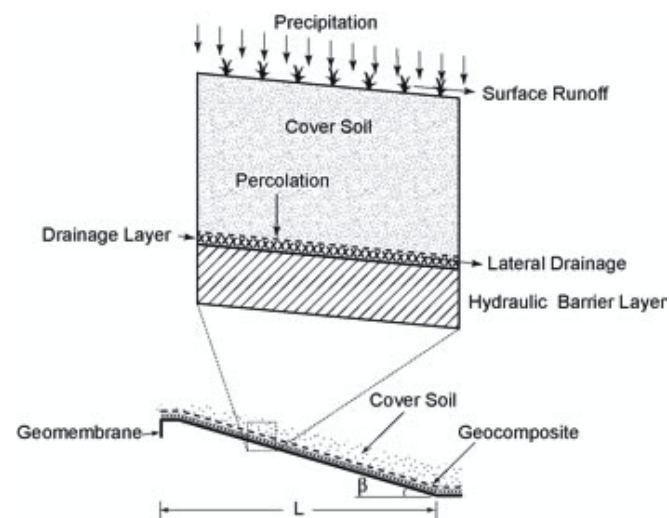


Figure 1. Disposition of precipitation in a typical final cover system.

While the quantity of water, Q_{out} , exiting from the drainage layer is calculated by Darcy's Law as follows:

$$Q_{out} = k_d \times i \times A = k_d \times i \times (t \times 1) = [k_d \times t] \times i = \theta \times i \quad (2)$$

Where k_d is the permeability of the drainage layer, and t is the thickness of the drainage layer, $i = \sin \beta$ is the hydraulic gradient, and $[k_d \times t]$ is defined as hydraulic transmissivity. The required transmissivity for the geocomposite drain can then be calculated

$$\theta_{req} = \frac{k_{veg} \cdot L}{i} = \frac{k_{veg} \cdot L}{\sin \beta} \quad (3)$$

The laboratory measured transmissivity of a geocomposite drain does not take into account the potential reduction factors during its design life. GRI-GC8 standard (2001) requires the allowable transmissivity being determined under simulated condition for 100-hour duration using the following formula:

$$\theta_{allow} = \theta_{100} \frac{1}{RF_{CR} \times RF_{CC} \times RF_{BC}} \quad (4)$$

where

θ_{allow} = allowable design transmissivity

θ_{100} = laboratory measured transmissivity determined under simulated conditions for 100-hour duration

RF_{CR} = reduction factor for compressive creep deformation

RF_{CC} = reduction factor for chemical clogging

RF_{BC} = reduction factor for biological clogging

A range of clogging reduction factors is provided by GRI-GC8. A higher reduction factor for biological clogging is recommended for landfill capping to account for the growth of biological organisms or by roots growing through the overlying soil and extending downward, through the geotextile filter layer, and into the drainage geonet core. The long term performance of a lateral drain requires a larger allowed transmissivity, $\theta_{allowed}$, than that obtained from the design equations, $\theta_{req'd}$ quantified by an overall safety of factor for drainage, as follows:

$$FS_{dc} = \frac{\theta_{allowed}}{\theta_{req'd}} \quad (5)$$

Combining equations (3), (4) and (5), the drainage safety factor, FS_{dc} , of the geocomposite drainage layer can then be calculated as follows:

$$FS_{dc} = \frac{\theta_{allow}}{\theta_{req}} = \theta_{allow} \frac{\sin \beta}{k \times L} = \theta_{100} \times \frac{1}{RF_{CR} \times RF_{CC} \times RF_{BC}} \times \frac{\sin \beta}{k \times L} \quad (6)$$

The selection of drainage FS -value is dependent upon the design life and criticality of the project, 2 – 3 is recommended by Giroud et al (2000), >10 for filtration and drainage by Koerner (2001).

Design Equations for Slope Stability

Surface water percolating through the vegetative soil layer over a barrier layer can produce seepage forces acting parallel to the slope if the soil layer saturates, as illustrated in Figure 2. The slope stability factor of safety for an infinite slope is given as:

$$FS = \frac{\text{Resisting Forces}}{\text{Driving Forces}} = \frac{\gamma_b d \cos \beta \tan \delta}{\gamma_b d \sin \beta + \gamma_w d \sin \beta} \quad (7)$$

$$= \frac{\gamma_b \tan \delta}{\gamma_{sat} \tan \beta} \approx 0.5 \frac{\tan \delta}{\tan \beta}$$

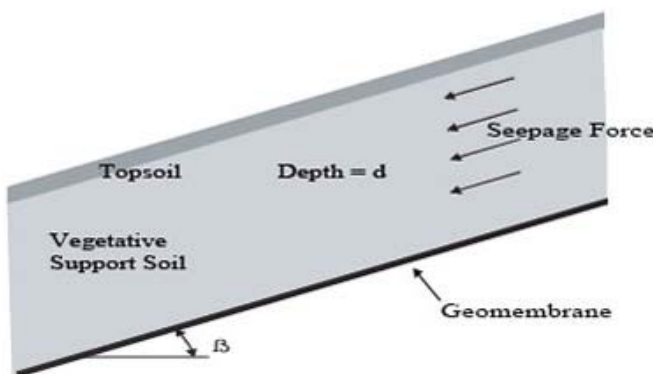


Figure 2. Seepage forces acting on side slope.

where γ_{sat} is the saturated unit weight of the soil and γ_b is the buoyant unit weight of the soil, and δ is the interface friction angle. When such seepage forces are eliminated by using a geocomposite drain with adequate transmissivity, the slope safety factor, FS , becomes:

$$FS = \frac{\tan \beta}{\tan \delta} \quad (8)$$

Thus, the use of a geocomposite drainage layer doubles the sliding factor of safety by preventing the formation of seepage forces in the cover soil. No engineering design would be technically sound and economic to allow such seepage forces in cover soil to occur.

Leakage Rate through Defects in a Geomembrane Liner

A composite final cover that creates a synergistic relationship between the geomembrane liner and an underlying soil liner provide the best barrier system to minimize liquid infiltration through any defects. Empirical modeling and field observations (Giroud and Badu-Tweneboah 1992) have resulted in the "Giroud" equation for estimating leakage through a hole in the geomembrane portion of a composite liner. The empirical equation takes the form of:

$$\frac{Q}{A} = n \cdot 0.976 \cdot C_{q0} \cdot [1 + 0.1 \cdot (h/t_s)^{0.95}] \cdot d^{0.2} \cdot h^{0.9} \cdot k_s^{0.74} \quad (9)$$

where C_{q0} is the contact quality factor, 0.21 for good contact and 0.15 for poor contact, "contact" here refers to the contact between the soil liner and the geomembrane. Good contact conditions correspond to a geomembrane installed with a few wrinkles as possible, on top of a low-permeability soil layer that has been adequately compacted and has a smooth surface; while a poor contact conditions corresponds to a geomembrane that has been installed with a certain number of wrinkles, and/or placed on a low-permeability soil that has not been well compacted and does not appear smooth. Q/A = rate of leakage through defect (m^3/s); n = number of defects, h = head of liquid on top of the geomembrane (m); t_s = thickness of the soil component of the composite liner (m); d = diameter of circular defect (m); and k_s = hydraulic conductivity of the underlying soil liner (m/s), as shown in Figure 3. Equation (9) has been incorporated into the US EPA HELP model used for predicting landfill leachate generation and leakage.

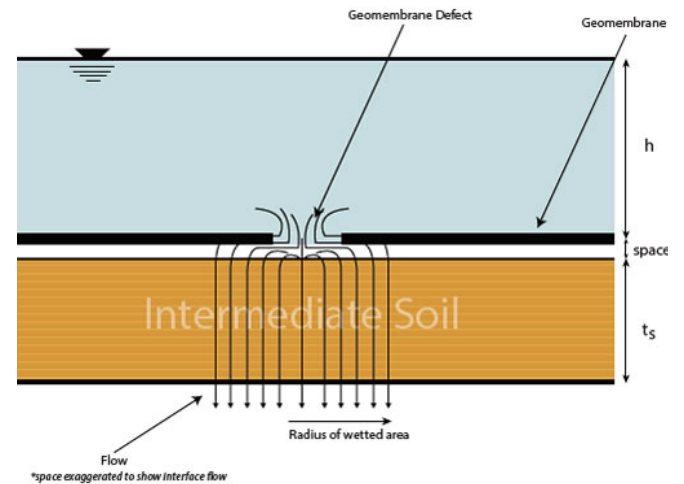


Figure 3. Composite liner variables.

Clearly leakage through a composite liner system increases with the following:

1. Increasing head
2. Decreasing soil liner thickness
3. Increasing soil liner permeability
4. Increasing area of defect in GM
5. Decreasing lack of good contact between the two liner components, and
6. Increasing number of defects in GM

CCR closure performance standards do not mandate a composite liner system closure. Leakage rate through defects in

a single geomembrane liner will be significantly greater than a composite liner. Thus, hydraulic head-control is critical to satisfy CCR closure performance standards for owner and operators to control, minimize or eliminate, to the maximum extent feasible, post-closure infiltration of liquids into the waste in flatter area of the closure.

REFERENCES

Giroud, J.P., Badu-Tweneboah, K., and Boneparte, R., (1992) "Rate of Leakage Through a Composite Liner Due to Geomembrane Defects", *Geotextiles and Geomembranes*, Vol. 11, No. 1, pp. 1-28.

Giroud, J.P., 1997, "Equations for Calculating the Rate of Liquid Migration Through Composite Liners Due to Geomembrane Defects", *Geosynthetics International*, Vol. 4, Nos. 3-4, pp.335-348.

Giroud, J.P., Zornberg, J.G. and Zhao, A., 2000, "Hydraulic design of geosynthetic and granular liquid collection layers", *Geosynthetics International*, Special Issue on Liquid Collection Systems, Vol. 7, Nos.4-6, pp. 285-380.

GRI-GC8 Standard (2001). Standard guide for determination of the allowable flow rate of a drainage geocomposite.

Richardson, G.N. and Zhao, A. (1998), "Designer's Forum, Composite drains for side slopes in landfill final covers", *Geotechnical Fabrics Report*, June/July, 1998, pp. 22-25.

Richardson, G.N., Giroud, J.P., and Zhao, A. (2002), "Lateral drainage design update-part 1", *Geotechnical Fabrics Report*, January/February, 2002, pp. 18-21.

Richardson, G.N., Giroud, J.P., and Zhao, A. (2002), "Lateral drainage design update-part 2", *Geotechnical Fabrics Report*, March, 2002, pp. 12-17.

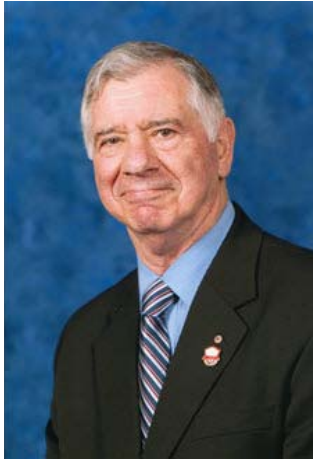
Soong, T.Y. and Koerner, R.M., 1997, "The Design of Drainage Systems Over Geosynthetically Lined Slopes", *Geosynthetics Research Institute*, Report #19.

Thiel, R.S., and Stewart, M.G., 1993, "Geosynthetic Landfill Cover Design Methodology and Construction Experience in the Pacific Northwest", *Geosynthetics'93*, Vancouver, pp. 1131-1144.

(Chris Kelsey / GSE Environmental, January 26, 2017, <http://www.geosynthetica.net/ccr-closure-geocomposite-drains-technote>)

ΔΙΑΚΡΙΣΕΙΣ ΕΛΛΗΝΩΝ ΓΕΩΜΗΧΑΝΙΚΩΝ

OPAL Winner Finds 'Foundation' for Success



Harry Poulos, 2017 OPAL winner in design

It's not difficult to see the civil engineering legacy of Harry Poulos.

Just scan the horizon.

Poulos, Ph.D., P.E., DSc.Eng., Dist.M.ASCE, is arguably the world's leading pile engineer. His work and research helped develop new methods for piled raft foundations that have made possible some of the tallest structures in the world, including the tallest, the Burj Khalifa in Dubai.

"You get a certain sense of pride in seeing something in the sky going up 800-plus meters and saying, 'I had a little bit to do with that,'" Poulos laughed.

"Every time I see the Burj Khalifa I get quite a kick out of it. We had a review role in that project. It was quite a collaborative effort with the designers, Hyder. It's always nice to be part of a cooperative team."

He characteristically downplayed his own role, but there's no overstating his contributions to the field of geotechnical engineering. ASCE has recognized Poulos as the 2017 Outstanding Project And Leaders award winner in design.

Poulos' career began at the University of Sydney, first as a student and then as an instructor. He steered clear of traditional structural engineering, finding himself more interested in what was happening underneath the structures, in the soil.

"I was intrigued by the uncertainty of it all," Poulos said. "The fact that no single project was ever the same. There was an element of novelty in every project that really fascinated me."

His Ph.D. work was in shallow soil foundations, but it was his research on deep soil that changed the industry. Poulos credits his time working with the late Ted Davis as being crucial to his development. Together, Poulos and Davis wrote *Elastic Solutions in Soil and Rock Mechanics*, published in 1974, and *Pile Foundation Analysis and Design* in 1980. Both remain a seminal works in pile foundations.

By the 1980s, Poulos' reputation was such that a lucrative consulting career beckoned. He joined the Coffey Group in 1989, where he served in various leadership positions for the next 26 years.

Beyond the Burj Khalifa, the impressive super-tall structures he has worked on include the Incheon 151 Tower in South Korea, the Emirates Project in Dubai, residential towers in Hong Kong, plus work in Israel, Malaysia, Singapore, Greece, Indonesia, and his home country of Australia. He continues teaching as an adjunct professor for the Hong Kong University of Science and Technology and professor emeritus at the University of Sydney.

"When I started off my research, I didn't know quite where it would end up," Poulos said. "In some ways I sort of stumbled into the area of deep soil foundations. It was almost a lucky accident that I got into it.

"I've just tried to enjoy applying theory to practice and finding that you can contribute in some way to real projects."

(Ben Walpole, ASCE News, March 8, 2017)

OPAL (Outstanding Projects And Leaders) Awards

The Society's annual Outstanding Projects And Leaders awards are among the highest tributes a civil engineer can achieve.

The [OPAL](#) goes beyond recognizing single accomplishments to honor its recipients for successful careers demonstrating leadership and achievement in one of five categories.

Construction - for innovation and excellence in construction of civil engineering project and/or programs.

Candidates in this category are senior level professionals whose primary responsibility is to oversee significant construction projects.

Design - for innovation and excellence in civil engineering design.

Nominees in Design are practitioners who are directly charged with hands-on design projects.

Education - for demonstrated excellence in furthering civil engineering education.

Candidates in the Education category are professors and deans whose careers are marked by achievements that direct or change the course of engineering education.

Government - for demonstrated leadership of public sector projects and/or programs.

Those chosen for honor in this category are civil engineers at work on public service construction projects or those who direct and oversee large government projects.

Management - for exceptional management skills in his/her professional career.

Nominees in this category are senior managers of an engineering organization, whose primary responsibility is to oversee and direct operations.

ΝΕΑ ΑΠΟ ΕΛΛΗΝΙΚΕΣ ΚΑΙ ΔΙΕΘΝΕΙΣ ΓΕΩΤΕΧΝΙΚΕΣ ΕΝΩΣΕΙΣ



Φωτογραφικός Διαγωνισμός «Φράγματα & Ταμιευτήρες»

Η Ελληνική Επιτροπή Μεγάλων Φραγμάτων (EEMF-GCOLD) με ιδιαίτερη χαρά ανακοινώνει τη διεξαγωγή Διαγωνισμού Φωτογραφίας με γενικότερο θέμα «Φράγματα & Ταμιευτήρες», στα πλαίσια του 3^{ου} Πανελληνίου Συνεδρίου Φραγμάτων & Ταμιευτήρων που θα διεξαχθεί 12-14 Οκτωβρίου 2017 στην Αθήνα.

Ο διαγωνισμός είναι ανοικτός για όλα τα μέλη της EEMF που θα συμμετάσχουν στις εργασίες του 3^{ου} Πανελληνίου Συνεδρίου Φραγμάτων & Ταμιευτήρων και διεξάγεται με τους ακόλουθους όρους.

ΟΡΟΙ ΔΙΑΓΩΝΙΣΜΟΥ

1. Θέμα του Διαγωνισμού

Το θέμα του διαγωνισμού είναι τα φράγματα και οι τεχνητοί ταμιευτήρες που σχηματίζονται από την κατασκευή των φραγμάτων. Οι φωτογραφίες μπορούν να απεικονίζουν στιγμές από την κατασκευή ή τη λειτουργία φραγμάτων, από πλημμύρες, υπερχειλίσεις κτλ. είτε από το φυσικό τοπίο που δημιουργείται με την κατασκευή του φράγματος και του ταμιευτήρα είτε από τη φύση ή τη ζωή γύρω ή μέσα σε αυτά. Οι φωτογραφίες μπορούν να απεικονίζουν το φράγμα ή τον ταμιευτήρα ή και τα δύο. Τα φράγματα και οι ταμιευτήρες θα πρέπει να βρίσκονται στην Ελλάδα.

2. Σκοπός του Διαγωνισμού

Ο σκοπός του διαγωνισμού είναι η καταγραφή, ανάδειξη και προβολή φωτογραφιών με θέμα τα φράγματα και ταμιευτήρες. Οι φωτογραφίες που θα επιλεγούν θα εκτεθούν σε έκθεση στα πλαίσια του 3ου Πανελληνίου Συνεδρίου Φραγμάτων & Ταμιευτήρων, καθώς και θα αναρτηθούν στην ιστοσελίδα της EEMF.

3. Προϋποθέσεις συμμετοχής στο Διαγωνισμό

Δικαίωμα συμμετοχής στο διαγωνισμό έχει κάθε φυσικό πρόσωπο το οποίο θα παρακολουθήσει τις εργασίες του 3^{ου} Πανελληνίου Συνεδρίου Φραγμάτων & Ταμιευτήρων.

Κάθε διαγωνιζόμενος μπορεί να υποβάλει έως πέντε (5) φωτογραφίες (προτάσεις).

Μαζί με τις φωτογραφίες θα πρέπει να υποβάλει τις ακόλουθες πληροφορίες για τις φωτογραφίες, συμπληρώνοντας το Έντυπο 2 του διαγωνισμού, το οποίο μπορεί να βρεθεί στο τέλος της παρούσας.

- Τον τίτλο της φωτογραφίας
- Την ονομασία του φράγματος ή/και ταμιευτήρα

- Τη γεωγραφική θέση του φράγματος ή/και ταμιευτήρα (περιοχή, συντεταγμένες ή υπόδειξη σε χάρτη)
- Το χρόνο λήψης της φωτογραφίας. Δεν υπάρχει περιορισμός στην ημερομηνία λήψης της φωτογραφίας, μπορούν δηλαδή να υποβληθούν φωτογραφίες που λήφθηκαν πριν την προκήρυξη του διαγωνισμού.
- Παρατηρήσεις σχετικά με τη φωτογραφία (προαιρετικό).

4. Κανονισμοί Πνευματικής Ιδιοκτησίας

Τα πνευματικά δικαιώματα των φωτογραφιών θα ανήκουν στους φωτογράφους. Με τη συμμετοχή στο διαγωνισμό γίνεται αποδεκτό από τους συμμετέχοντες ότι οι διοργανωτές του διαγωνισμού έχουν το δικαίωμα εκτύπωσης, έκθεσης, αναπαραγωγής, ανάρτησης σε ιστοσελίδα, δημοσίευσης των φωτογραφιών και άλλης αξιοποίησης όπως αναγράφεται στους όρους του διαγωνισμού.

Ο κάθε διαγωνιζόμενος θα πρέπει να είναι και ο φωτογράφος των υποβληθεισών φωτογραφιών, δηλώνοντάς το σχετικά.

Ο κάθε διαγωνιζόμενος είναι υπεύθυνος για την υποβολή δήλωσης πνευματικής ιδιοκτησίας, σύμφωνα με τις ισχύουσες διατάξεις της Ελληνικής Νομοθεσίας.

Η EEMF δεν φέρει ουδεμία ευθύνη σε περίπτωση ψευδούς υποβολής δήλωσης καθώς μοναδικός υπεύθυνος για την εγκυρότητα της πνευματικής ιδιοκτησίας είναι ο κάθε διαγωνιζόμενος.

5. Βραβεία

Θα απονεμηθούν τα παρακάτω βραβεία:

1ο Βραβείο: 300 ΕΥΡΩ

2ο Βραβείο: 150 ΕΥΡΩ

3ο Βραβείο: 100 ΕΥΡΩ

Επίσης θα απονεμηθούν και δέκα (10) έπαινοι. Τα βραβεία και οι έπαινοι θα επιδοθούν κατά τη διάρκεια του 3ου Πανελληνίου Συνεδρίου Φραγμάτων & Ταμιευτήρων.

6. Κριτική Επιτροπή

Η κριτική επιτροπή είναι τριμελής με την ακόλουθη σύνθεση:

- Χρήστος Δήμου, Δρ. Πολ. Μηχανικός, ΔΕΗ/ΔΥΗΠ
- Μαρία Μπενίση, Τεχνικός Γεωλόγος MSc, DIC, Αττικό Μετρό
- Γιώργος Σαχίνης, ΕΥΔΑΠ

7. Επίσημη διεύθυνση Διαγωνισμού

ΕΛΛΗΝΙΚΗ ΕΠΙΤΡΟΠΗ ΜΕΓΑΛΩΝ ΦΡΑΓΜΑΤΩΝ
(ΜΕΛΟΣ ΤΗΣ ΔΙΕΘΝΟΥΣ ΕΠΙΤΡΟΠΗΣ ΜΕΓΑΛΩΝ ΦΡΑΓΜΑΤΩΝ)
μέσω ΔΕΗ - ΔΥΗΠ ΑΓΗΣΙΛΑΟΥ 56-58 104 36 ΑΘΗΝΑ
Τηλ: 210-3355328 Fax: 210 - 5241223, Η/Δ: eemf@eefl.gr

8. Υποβολή ερωτήσεων

Ερωτήσεις αναφορικά με την ερμηνεία των όρων του διαγωνισμού μπορούν να υποβληθούν με e-mail στην παραπάνω διεύθυνση.

9. Χρονοδιάγραμμα Διαγωνισμού

Το χρονοδιάγραμμα του Διαγωνισμού είναι ως εξής:

- Ημερομηνία προκήρυξης του Διαγωνισμού 15/06/2017
- Τελευταία ημερομηνία υποβολής ερωτήσεων 15/07/2017
- Προθεσμία υποβολής προτάσεων (φωτογραφιών) 15/09/2017 και ώρα 12 μεσημέρι

iv. Επιλογή φωτογραφιών από την Κριτική επιτροπή και γνωστοποίηση των αποτελεσμάτων στους διαγωνιζόμενους μέχρι 01/10/2017

Οι διοργανωτές διατηρούν το δικαίωμα τροποποίησης των ημερομηνιών που αναφέρονται πιο πάνω, αν αυτό θεωρηθεί αναγκαίο για οποιοδήποτε λόγο.

10. Υποβολή Συμμετοχής στο Διαγωνισμό

Οι διαγωνιζόμενοι θα πρέπει να αποστείλουν τις προτάσεις τους στην επίσημη διεύθυνση του διαγωνισμού μέχρι την προθεσμία υποβολής που αναφέρεται πιο πάνω.

Οι διαγωνιζόμενοι θα πρέπει να χρησιμοποιήσουν αντί του ονόματός τους εξαψήφιο κωδικό αριθμό της επιλογής τους.

Οι φωτογραφίες που θα υποβληθούν θα πρέπει να δοθούν σε ψηφιακή μορφή jpg σε ψηφιακό δίσκο (CD), με ελάχιστη ανάλυση (resolution) 300dpi και μέγεθος τουλάχιστον 4 megapixel. Εκτυπωμένες φωτογραφίες δεν θα γίνονται δεκτές.

Οι φωτογραφίες πρέπει να είναι φυσικές και να μην έχουν υποστεί ψηφιακή τροποποίηση. Φωτογραφίες που δεν φαίνονται φυσικές ή έχουν υποστεί ψηφιακή τροποποίηση δεν θα γίνονται δεκτές.

Δεν επιτρέπεται να υπάρχουν υπογραφές, σημειώσεις ή υδατογραφήματα στις φωτογραφίες.

Στο CD θα πρέπει να αναγράφεται ο εξαψήφιος κωδικός αριθμός του κάθε διαγωνιζόμενου.

Το όνομα κάθε αρχείου φωτογραφίας θα πρέπει να περιλαμβάνει τον εξαψήφιο αριθμό και τον αύξοντα αριθμό της υποβολής, σύμφωνα με το συμπληρωμένο πίνακα του Έντυπου 2, π.χ. 123456-1.jpg (για την πρώτη φωτογραφία της υποβολής του διαγωνιζόμενου που επέλεξε τον εξαψήφιο αριθμό 123456).

Η υποβολή θα γίνεται σε κλειστό φάκελο στο εξωτερικό του οποίου θα αναγράφεται:

Διαγωνισμός Φωτογραφίας «Φράγματα και Ταμιευτήρες»

Ο φάκελος θα πρέπει να περιέχει:

- i. Κλειστό σφραγισμένο υποφάκελο που θα περιέχει συμπληρωμένο το Έντυπο 1 και ο οποίος εξωτερικά θα γράφει ΜΟΝΟ τον εξαψήφιο κωδικό αριθμό του διαγωνιζόμενου και τον τίτλο ΕΝΤΥΠΟ 1, π.χ. 123456 – ΕΝΤΥΠΟ 1
- ii. Το CD με τις φωτογραφίες σύμφωνα με τις προδιαγραφές της προηγούμενης παραγράφου
- iii. Συμπληρωμένο το Έντυπο 2 μαζί με το CD.

11. Συμμετοχή στο Διαγωνισμό

Η συμμετοχή στο διαγωνισμό είναι δωρεάν, με μόνη προϋπόθεση ο διαγωνιζόμενος να παρακολουθήσει τις εργασίες του 3^{ου} Πανελληνίου Συνεδρίου Φραγμάτων & Ταμιευτήρων.

<http://www.fragmata2017.gr/files/PhotoContestDams2017.pdf>



Για τις παλαιότερες καταχωρήσεις περισσότερες πληροφορίες μπορούν να αναζητηθούν στα προηγούμενα τεύχη του «περιοδικού» και στις παρατιθέμενες ιστοσελίδες.



Call for Papers: In situ tests in geotechnical engineering

Dear Colleague,

You are warmly invited to propose a paper for the themed issue of **Geotechnical Research** on *In situ tests in geotechnical engineering*, championed by Myint Win Bo (Bo & Associates Inc., Canada). Please [submit](#) an abstract of the article you would like to write by **31st October 2017**.

In situ testing is used to acquire data to determine geotechnical parameters or interpret geotechnical parameters which can be used in geotechnical analyses and design. Geotechnical parameters could be classification parameters or strength and deformation parameters. Examples of in situ testing include the standard penetration test, cone penetration test, dilatometer test, pressuremeter test, in situ hydraulic conductivity test and nuclear gauge.

Interested academics, researchers, practitioners, engineers and scientists are requested to participate and showcase their research output and industrial case studies on in situ testing in soils and rocks for the purpose of direct measurement of in situ soil and rock parameters or acquiring data so as to interpret geotechnical parameters indirectly. Submissions could be based on field or experimental laboratory testing and modelling as well as case studies on successful application of in situ testing equipment.

Indexed in 2015 Scopus SJR Ranking, the Emerging Sources Citation Index, and the Directory of Open Access Journals, **Geotechnical Research** aims to disseminate knowledge on any aspect of modern geotechnics, through the Gold Open Access model (Funded by Article Publication Charges (APCs)) to engineers worldwide.

To learn more about the themed issue and for a **list of topics**, please [download the Call for Papers](#). For more information on the journal, please [visit the website](#).

Thank you and kind regards,

2nd International Symposium on Coastal and Offshore Geotechnics (ISCOG 2017) & 2nd International Conference on Geo-Energy and Geo-Environment (GeGe2017) 5-7 July 2017, Zhejiang University, China www.issmge.org/events/iscoq-2017-gege-2017

Two crucial global challenges facing the 21st century are exploration of energy (including offshore wind and deep-water methane hydrate) and management of geo-environment, both of which are essential for building a sustainable future. To provide a platform for sharing scientific breakthroughs in sustainable geotechnical solutions to energy production and geo-environment management, Zhejiang University has successfully organized the 1st International Symposium on Coastal and Offshore Geotechnics (**ISCOG 2012**) in Hangzhou, and jointly organized the 1st International Conference on Geo-Energy and Geo-Environment (**GeGe2015**) with the Hong Kong University of Science and Technology.

Considering the two international conferences are highly complementary, we are arranging the 2nd **ISCOG & GeGe2017** events in parallel in 2017 at Zhejiang University (China), with the specific aim of enhancing multi-disciplinary interactions in the areas related to energy and geo-environment management. This combined event (**ISCOG2017 & GeGe2017**) is supported by the ISSMGE. In the conference, two parallel programmes will be offered, but also with substantial common plenary sessions and keynotes by prominent speakers.

The presentations will include a re-run of the 2016 Rankine Lecture by Professor Richard Jardine from Imperial College, as well as a re-run of the 2017 Terzaghi Lecture by Professor Kerry Rowe from Queen's University.

Contact person: Yi Hong
Address: 866 Yuhangtang Road, Hangzhou, Zhejiang Province, China
Phone: +86 13758906685
Email: yi_hong@zju.edu.cn

isfog2017_gege2017@zju.edu.cn



TRANSOILCOLD2017 The 3rd International Symposium on Transportation Soil Engineering in Cold Regions 5 -7 July 2017, Guide City, China, <http://transoilcold2017.applinzi.com/index.php>

10th World Congress on Water Resources and Environment "Panta Rhei", 5-9 July 2017, Athens, Greece, <http://ewra2017.ewra.net>

GeoMEast2017, 15 - 19 July 2017, Sharm El-Sheik, Egypt, www.geomeast2017.org

3rd International Conference on Performance-based Design in Earthquake Geotechnical Engineering (PBD-III), July 16 - 19, 2017, Vancouver, Canada, <http://pbdiiivancouver.com>

ICTUS17 The 2017 International Conference on Tunnels and Underground Spaces, 28 August 2017 - 1 September 2017, Seoul, Korea, www.i-asem.org/new_conf/asem17.htm

International Symposium on Coupled Phenomena in Environmental Geotechnics, 6-8 September 2017, Leeds, United Kingdom, <http://tinyurl.com/cpeg2017>



<https://brownfieldbriefing.com/risk-remediation-2017?ls=lnk>

Regulatory & Planning Updates & Practical Solutions To Deliver Risk-Based, Robust & Achievable Contaminated Land Development

Developing a time- and cost-effective remediation strategy that is "fit for purpose" and satisfies new planning and regulatory requirements is vital in successfully developing brownfield land. Where contamination is present, having confidence in the information provided by a rigorous and justifiable risk assessment is essential to avoid unnecessary costs. Setting realistic remediation targets and evaluating all of the remedial options available, including new technologies, can save both time and money, whilst achieving greater certainty of results.

Developing on brownfield sites is not easily achieved. Barriers such as complicated or unclear ownership makes land purchase difficult, add-in physical obstacles such as contamination and lack of infrastructure, and this significantly affects the viability of brownfield sites, hindering or preventing their redevelopment. Many formerly-used sites are considered unviable by developers because of the high risks, costs and complexities associated with them, meaning that bringing brownfield land back into re-use is costly, has long timescales and is fraught with uncertainties.

This popular annual event, held in London on 13th & 14th September will bring together regulators, consultants, remediation contractors and other industry experts working across the whole of the brownfield sector to discuss a wide range of issues within contaminated land risk assessment and remediation. effective risk assessment and remediation. The inter-linked nature of these two topics means that delegates attending both days of the conference will benefit from the most holistic view, however it is also possible to attend just day One or Two.

Join us and benefit from hearing regulatory updates and sharing first-hand experiences with your peers, enabling you to develop practical and cost-effective solutions to current remediation challenges.



19th International Conference on Soil Mechanics and Geotechnical Engineering, 17 - 22 September 2017, Seoul, Korea, www.icsmge2017.org

AfriRock 2017, 1st African Regional Rock Mechanics Symposium, 2 - 7 October 2017, Cape Town, South Africa, www.saimm.co.za/saimm-events/upcoming-events/afrirock-2017

Geotechnique Symposium in Print 2017 Tunnelling in the Urban Environment, <http://www.icevirtuallibrary.com/pb-assets/Call%20for%20Papers/Geo-Symposium-CFA-AW.pdf>

HYDRO 2017 Shaping the Future of Hydropower, 9-11 October 2017, Seville, Spain, hydro2017@hydropower-dams.com

GeoAfrica 2017 3rd African Regional Conference on Geosynthetics, 9 - 13 October 2017, Morocco, <http://geoafrica2017.com>

3ο Πανελλήνιο Συνέδριο Φραγμάτων και Ταμιευτήρων - Διαχείριση Έργων και Προοπτικές Ανάπτυξης, 12 - 14 Οκτωβρίου 2017, Αθήνα, www.fragmata2017.gr

4th International Conference on Long-Term Behaviour and Environmentally Friendly Rehabilitation Technologies of Dams, 17-19 October 2017, Tehran, Iran, www.ltb2017.ir/en

The 15th International Conference of International Association for Computer Methods and Advances in Geomechanics, 18- 22 October 2017, Wuhan, Hubei Province, China, www.15iacmaq.org

XIII International Conference "Underground Infrastructure of Urban Areas 2017", 24-26 October 2017, Wroclaw, Poland, <http://uiua.pwr.edu.pl/?lang=en>

ISAUG 2017 2nd International Symposium on Asia Urban GeoEngineering, 24-27 November 2017, Changsha, China, www.isaug2017.org

SIFRMEG 2017 Shaoxing International Forum on Rock Mechanics and Engineering Geology, October 28-29, 2017, <http://forum.hmkj.com.cn/index.php/Index/show/tid/20>



11ο Συνέδριο «Ελληνική Γλώσσα και Ορολογία» 9-11 Νοεμβρίου 2017, Αθήνα

Αφιερωμένο στον **Κωστή Παλαμά**

Η Ελληνική Εταιρεία Ορολογίας (ΕΛΕΤΟ), σε συνεργασία με το Εθνικό και Καποδιστριακό Πανεπιστήμιο Αθηνών (ΕΚΠΑ), το Αριστοτέλειο Πανεπιστήμιο Θεσσαλονίκης (ΑΠΘ), το Πανεπιστήμιο Κύπρου (ΠΚ), το Τεχνικό Επιμελητήριο Ελλάδας (ΤΕΕ), τον Ελληνικό Οργανισμό Τυποποίησης (ΕΛΟΤ), τον Οργανισμό για την Διάδοση της Ελληνικής Γλώσσας (ΟΔΕΓ) και άλλους φορείς που θα ανακοινωθούν στην ιστοσελίδα

του Συνεδρίου, διοργανώνει το **11ο Συνέδριο "Ελληνική Γλώσσα και Ορολογία"**. Το Συνέδριο θα διεξαχθεί στην **Αθήνα** στις **9-11 Νοεμβρίου 2017**.

Σκοπός του Συνεδρίου είναι η παρουσίαση αφενός της σημερινής κατάστασης της ελληνικής γλώσσας στην ορολογική της διάσταση και αφετέρου μεθόδων, πρακτικών και εργαλείων της σύγχρονης επιστήμης της Ορολογίας και της εφαρμογής τους στην ελληνική γλώσσα – μονογλωσσικά και/ή διαγλωσσικά – για την προώθηση της ορολογικής έρευνας και τη συμβολή στον σύγχρονο ορολογικό εμπλουτισμό της ελληνικής γλώσσας.

Θεματολόγιο του Συνεδρίου

1 Γλωσσολογικές-οντολογικές αρχές Ορολογίας

Αρχές της γλώσσας και της λογικής που υιοθετούνται, διατυπώνονται και εφαρμόζονται στην Ορολογία. Η ορολογία ως διεπαφή ανάμεσα στη γλώσσα και στη γνώση. Μέθοδοι, μηχανισμοί και κανόνες οροδοσίας που προκύπτουν από την ενδογλωσσική ή την διαγλωσσική εξέταση κατασημάνσεων (όρων και ονομάτων) και ορισμών εννοιών. Θεωρητική, συγχρονική και/ή διαχρονική εξέταση όρων σε μονογλωσσικό και/ή πολυγλωσσικό περιβάλλον.

2 Διδακτική και Ορολογία

Διδακτική της Ορολογίας. Προπτυχιακά και μεταπτυχιακά μαθήματα και/ή σεμινάρια Ορολογίας. Μαθησιακά θέματα Ορολογίας. Ορολογικές πλευρές της διδασκαλίας μαθημάτων ειδικών θεματικών πεδίων. Έννοιες και όροι της Διδακτικής.

3 Ορολογία συγκεκριμένων θεματικών πεδίων – Λεξικογραφικές και ορογραφικές μελέτες

Συγχρονική και/ή διαχρονική θεώρηση ορολογίων και ορολογικών προβλημάτων συγκεκριμένων θεματικών πεδίων. Συστήματα όρων σε συγκεκριμένα θεματικά πεδία σε σχέση με αντίστοιχα συστήματα εννοιών. Λεξικογραφικές και ορογραφικές μελέτες σε συγκεκριμένα θεματικά πεδία.

4 Ορολογικοί πόροι

Ειδικά ερμηνευτικά ή πολύγλωσσα λεξικά, έντυπα ή ηλεκτρονικά, τοπικά ή επιγραμμικά/διαδικτυακά. Ορολογικές συλλογές ή βάσεις όρων που περιέχουν κατασημάνσεις, ορισμούς εννοιών και άλλες ορολογικές πληροφορίες. Σώματα ειδικών κειμένων και διάθεσή τους για έρευνα και υποστήριξη ορολογικών πόρων. Εφαρμογή των νέων τεχνολογιών στην ορολογική πράξη και στην παροχή ορολογικών υπηρεσιών.

5 Τυποποίηση ορολογίας

Ενδογλωσσική επικύρωση και τυποποίηση όρων με καθιέρωση προτιμώμενων και αποδεκτών όρων ως έγκυρων όρων. Διεθνοποίηση εννοιών και διαγλωσσική αντιστοίχιση, επικύρωση και τυποποίηση των ισοδύναμων όρων. Προτάσεις όρων για επικύρωση και τυποποίηση. Τυποποίηση κειμένων ειδικών γλωσσών.

6 Ορολογία και μετάφραση

Ο ρόλος των όρων στη θεωρία και πράξη της μετάφρασης. Εφαρμογή των αρχών της Ορολογίας στη μετάφραση. Η εννοιοστρεφής διαγλωσσική αντιστοίχιση και «ισοδυναμία» όρων μεταξύ πρωτοτύπου και μεταφράσματος έναντι της λεξιστρεφούς «μετάφρασης» όρων. Η μετάφραση με την βοήθεια ορολογικών πόρων από το Διαδίκτυο. Έννοιες και όροι της μεταφρασεολογίας.

7 Διάχυση και χρήση των όρων – Ορολογική πολιτική και ρύθμιση

Τρόποι και μέσα διάδοσης ειδικών όρων και ορολογίων. Ενδοπεδικά και διαπεδικά ζητήματα ορολογικής ενημέρωσης.

Ρυθμιστικά εργαλεία ορολογικής πολιτικής (δημοσιεύματα, νομοθετήματα, προδιαγραφές, πρότυπα).

8 Δραστηριότητα φορέων και οργάνων Ορολογίας – Το Ελληνικό Δίκτυο Ορολογίας (ΕΔΟ)

Δραστηριότητες παραγωγής, συλλογής, επεξεργασίας, δημοσιοποίησης και διάθεσης όρων και παροχής ορολογικών υπηρεσιών από εθνικούς, περιφερειακούς και/ή παγκόσμιους φορείς και όργανα (οργανισμούς, εταιρείες, ενώσεις, επιτροπές, ομάδες). Διοργανώσεις εκδηλώσεων Ορολογίας. Θα περιληφθεί ειδική συνεδρία για το Ελληνικό Δίκτυο Ορολογίας (ΕΔΟ), την ανάπτυξή του και τις δραστηριότητές του.

Γλώσσες

Επίσημες γλώσσες του Συνεδρίου είναι η **ελληνική** και η **αγγλική**.

Πληροφορίες

Οργανωτική Επιτροπή: τηλ. +30 6974321009, ηλ-ταχ. valeonti@otenet.gr

Γραμματεία του Συνεδρίου: τηλ. +30 210 9323243, +30 6977529164, ηλ-ταχ. pinelpap@otenet.gr

Ιστότοπος: <http://www.eleto.gr/gr/Conference11.html>.



PARIS 2017 AFTES International Congress "The value is Underground", 13-16 November 2017, Paris, France, www.aftes2017.com

World Tunnel Congress 2018 "The Role of Underground Space in Future Sustainable Cities", 20-26 April 2018, Dubai, United Arab Emirates, www.wtc2018.ae



EUROCK 2018

22-26 May 2018, Saint Petersburg, Russia

Contact Person: Prof. Vladimir Trushko
Address: 21-st line V.O., 2
199106 St. Petersburg
Russia
Telephone: +7 (812) 328 86 71
Fax: +7 (812) 328 86 76
E-mail: trushko@spmi.ru



16th European Conference on Earthquake Engineering (16thECEE), 18-21 June 2018, Thessaloniki, Greece, www.16ecee.org

CPT'18 4th International Symposium on Cone Penetration Testing, 21-22 June 2018, Delft, Netherlands, www.cpt18.org



NUMGE 2018

9th European Conference on Numerical Methods in Geotechnical Engineering 25-27 June 2018, Porto, Portugal www.numge2018.pt

The European Regional Technical Committee ERTC7 of the International Society for Soil Mechanics and Geotechnical Engineering (ISSMGE) and the Portuguese Geotechnical Society (SPG) have the pleasure of inviting you to attend the 9th NUMGE Conference on Numerical Methods in Geotechnical Engineering in Porto, Portugal, 25-27 June 2018.

This conference is the ninth in a series of conferences on Numerical Methods in Geotechnical Engineering organized by the ERTC7 under the auspices of the International Society for Soil Mechanics and Geotechnical Engineering (ISSMGE). Locally the organization has been assigned to SPG.

The first conference was held in 1986 in Stuttgart, Germany and the series continued every four years (1990 Santander, Spain; 1994 Manchester, United Kingdom; 1998 Udine, Italy; 2002 Paris, France; 2006 Graz, Austria; 2010 Trondheim, Norway; 2014 Delft, The Netherlands).

The conference provides a forum for exchange of ideas and discussion on topics related to numerical modelling in geotechnical engineering. Both senior and young researchers, as well as scientists and engineers from Europe and overseas, are invited to attend this conference to share and exchange their knowledge and experiences.

Conference Themes

Regarding the theoretical themes, the following are pointed out, among others:

- Constitutive modelling and numerical implementation
- Numerical algorithms and theoretical aspects
- Finite element, discrete element and other numerical methods. Coupling of diverse methods
- Reliability and probability analysis
- Large deformation – large strain analysis
- Artificial intelligence and neural networks
- Ground flow, thermal and coupled analysis
- Unsaturated soil mechanics
- Earthquake engineering, soil dynamics and soil-structure interactions
- Rock mechanics

Practical applications namely related to the following types of works:

- Application of numerical methods in the context of the Eurocodes
- Shallow and deep foundations
- Slopes and cuts
- Supported excavations and retaining walls
- Embankments and dams
- Tunnels and caverns (and pipelines)
- Ground improvement and reinforcement
- Offshore geotechnical engineering
- Propagation of vibrations and mitigation measures

For scientific information, please contact:

Organising Committee
Tel. +351 220 413 747
Email numge2018@fe.up.pt
Address

NUMGE2018

Civil Engineering Department, Faculty of Engineering, University of Porto
Rua Dr. Roberto Frias - 4200-465 Porto, Portugal

For practical information, please contact:

Lurdes Catalino - Conference Secretariat
Tel. +351 22 204 3573
Email lurdes.catalino@abreu.pt
Address

Abreu Events - Porto Office

Av. dos Aliados, nº 207 - 4000-067 Porto



RockDyn-3 - 3rd International Conference on Rock Dynamics and Applications, 25-29 June 2018, Trondheim, Norway, www.rocdyn.org

GeoChina 2018 - 5th GeoChina International Conference Civil Infrastructures Confronting Severe Weathers and Climate Changes: From Failure to Sustainability, July 23-25, HangZhou, China, <http://geochina2018.geoconf.org>

UNSAT2018 The 7th International Conference on Unsaturated Soils, 3 - 5 August 2018, Hong Kong, China, www.unsat2018.org



SAHC 2018

11th INTERNATIONAL CONFERENCE ON STRUCTURAL ANALYSIS OF HISTORICAL CONSTRUCTIONS

11th International Conference on Structural Analysis of Historical Constructions "An interdisciplinary approach" 11-13 September 2018, Cusco, Perú <http://sahc2018.com>

The International Conference on Structural Analysis of Historical Constructions (SAHC 2018) will be an event that continues the successful bi-annual series of conferences that started back in 1995. SAHC conferences are highly prestigious international events that allow sharing and dissemination of research and practice, as well as networking in this exciting field.

The SAHC 2018 will be organized by the Pontificia Universidad Católica del Perú and will take place from September 11 to 13, 2018 in Cusco, Perú. The theme of the conference will be "An Interdisciplinary Approach" which emphasizes the importance of the involvement of a variety of disciplines in the task of conserving and restoring heritage buildings.

Motivation

The technological advances achieved in the past decades

enabled great developments and uncovered new challenges in the field of structural analysis of historical and archaeological constructions. Progress also made evident that accuracy and robustness of results rely on an *interdisciplinary approach*, where different areas of expertise from architecture to engineering work together towards a common understanding of the history, the material, the structure, the analysis, and the intervention. Bearing this in mind, the 11th edition of SAHC, in 2018, aims at bringing up to discussion the new knowledge developed in the different disciplines involved in conservation, retrofit and management of historical and archaeological constructions. We welcome you to join this international event where we can all come together, to discuss and exchange insights, concerning recent advances and challenges we all face in research or professional practice in this field.

Topics

- History of construction and building technology.
- New technologies and techniques.
- Inspection, non-destructive and laboratory testing.
- Numerical modeling and structural analysis.
- Vulnerability and risk analysis regarding natural and man-made hazards.
- Seismic analysis and retrofit.
- Repair and strengthening techniques.
- Assessment and intervention of archaeological heritage.
- Durability and sustainability.
- Management of heritage structures and conservation strategies.
- Structural health monitoring.
- Interdisciplinary projects and case studies.

For more information on how to become a sponsor of this event please contact the Conference Secretariat at sahc2018@pucp.edu.pe



11th International Conference on Geosynthetics (11ICG), 16 - 20 Sep 2018, Seoul, South Korea, www.11icg-seoul.org

CHALK 2018 Engineering in Chalk 2018, 17-18 September 2018, London, U.K., www.chalk2018.org

ARMS10 - 10th Asian Rock Mechanics Symposium, ISRM Regional Symposium, 29 October - 3 November 2018, Singapore, www.arms10.org



**Tunnels and Underground Cities:
Engineering and Innovation meet Archaeology,
Architecture and Art
and**

ITA - AITES General Assembly and World Tunnel Congress

3-9 May 2019 · Naples · Italy

www.wtc2019.com

Società Italiana Gallerie (SIG) welcomes you to the World Tunnel Congress and ITA - AITES General Assembly in Naples, Italy.

Don't miss out on an opportunity to add this memorable event to your calendar from **May 3rd to May 9th 2019!**

WTC 2019 will be held in a spectacular venue, the famous "Mostra D'Oltremare", one of the main conference hubs in Italy. Its size, architectural properties and services make it a large multi-purpose centre with the ability to host congress rooms and an exhibition in the same area.

Combining a unique location and a great city that is fully representative of the 'Italian lifestyle' with archeology, architecture, art, touristic attractions and of course, tunnelling. Not to mention, important underground works built recently in a unique and complex geology, giving impressive examples of how important and attractive underground works were built. **The Toledo Metro Station on Line 1, received the 2015 ITA award for "Innovative Use of Underground Space"**. It is a unique example of a decentralized museum, offering dynamic fruition of artists' creations, with an opportunity for citizens to travel an open artistic route.

SIG expresses its support, enthusiasm and strong willingness to host the WTC 2019 in Naples, as well as, city authorities who will be honoured and will do their utmost best, to ensure the delegates' expectations.

The conference will offer the traditional topics on design and construction of underground works, focusing on **tunnelling, engineering and innovation**. In addition, to combining some unusual topics suggested by the Neapolitans, which are true Italian trademarks, such as history (**Archeology**), design (**Architecture**) and genius & creativity (**Art**).

The Neapolitan area is the cradle of underground works, that date back to the Roman period, while at the same time, an innovative and future-oriented city. Therefore, WTC delegates will enjoy visiting the tunnelling history from the Roman period, to the newest award winning metro station. Moreover, thanks to its morphologic structure, its long experience in building tunnels, and underground works dating back 5,000 years ago, Italy is able to offer a wide variety of examples forming the Triple "A" : **Archaeology, Architecture and Art**. Technical visits will include a visit to the longest underground railway in the world:

- NAPLES: Borbonic Tunnel, Greek-Roman Aqueduct, the underground remains of the Roman Theatre
- ROME: Line C - the 'Archeological' Metro
- BRENNER: Brenner Base Tunnel

Last but not least, WTC 2019 Naples will be an opportunity to organize special educational sessions. A number of WTC sessions will be broadcasted to universities and cultural associations, expanding the audience that can benefit from the knowledge shared by international experts.

Even the social program will be an opportunity to experience the archaeological sites of this beautiful setting.

Topics

- Strategic use of underground space for resilient cities
- Urban tunnels

- Long and deep tunnels
- Innovation in underground engineering, materials and equipment
- Safety in underground construction
- Environment sustainability in underground construction
- Public communication and awareness
- Risk management, contracts and financial aspects
- Geological and geotechnical information and requirements for project implementation
- Archeology, Architecture and Art in underground construction
- Ground Improvement in underground constructions

Information

SIG · Italian Tunnelling Society
Via E. Breda, 28 c/o Italferr SpA · 20126 Milano
www.societaitalianagallerie.it

Professional Congress Organizer

AIM Group International · Milan Office
Via G. Ripamonti, 129 · 20141 Milano
wtc2019@aimgroup.euwww.aimgroupinternational.com



7 ICEGE 2019

**International Conference on Earthquake
Geotechnical Engineering
17 - 20 June 2019, Rome, Italy**

Organizer: TC203 and AGI (Italian Geotechnical Society)
Contact person: Susanna Antonielli
Address: AGI - Viale dell' Università 11, 00185, Roma, Italy
Phone: +39 06 4465569
Fax: +39 06 44361035
E-mail: agi@associazionegeotecnica.it



ISDCG 2019

**7th International Symposium on Deformation
Characteristics of Geomaterials
26 - 28 June 2019, Glasgow, Scotland, UK,**

The Technical Committee 101 of the ISSMEG is pleased to announce the organisation of the 7th International Symposium on Deformation Characteristics of Geomaterials (ISDCG) in 2019, in Glasgow, UK. The symposium is co-organised by the University of Strathclyde in Glasgow, the University of Bristol, and the Imperial College in London.

Building on the success of the previous Symposia organised in Sapporo (Japan) Japan in 1994, Torino (Italy) in 1999, Lyon (France) in 2003, Atlanta (US) in 2008, Seoul (Korea) in 2011 and Buenos Aires (Argentina) in 2015, the 7th ISDCG will equally follow both its traditions and active promotion of new technical elements to maintain it as one of

the most popular and vibrant events within the geotechnical community. The technical core themes will focus on: (i) advanced laboratory geotechnical testing; (ii) application of advanced laboratory testing in research, site characterisation, and ground modelling; (iii) application of advanced testing to practical geotechnical engineering. In addition to these traditional topics, sub-themes will include cutting-edge techniques and approaches, for example experimental micro-mechanics, non-invasive monitoring systems, nano and micro-sensors, new sensing technologies. A key goal is to engage with the full spectrum of geotechnical specialists, from early career engineers and researchers through to world leading experts.



**14th ISRM International Congress
20-27 September 2019, Foz de Iguaçu, Brazil**

Contact Person: Prof. Sergio A. B. da Fontoura
E-mail: fontoura@puc-rio.br



**The 17th European Conference on
Soil Mechanics and Geotechnical Engineering
"Geotechnical Engineering,
foundation of the future"
1st - 6th September 2019, Reykjavik Iceland
www.ecsmge-2019.com**

The theme of the conference embraces all aspects of geotechnical engineering. Geotechnical engineering is the foundation of current as well as future societies, which both rely on complex civil engineering infrastructures, and call for mitigation of potential geodangers posing threat to these. Geotechnical means and solutions are required to ensure infrastructure safety and sustainable development. Those means are rooted in past experiences enhanced by research and technology of today.

At great events such as the European Geotechnical Conference we should: Spread our knowledge and experience to our colleagues; Introduce innovations, research and development of techniques and equipment; Report on successful geotechnical constructions and application of geotechnical design methods, as well as, on mitigation and assessment of geohazards and more.

Such events also provide an opportunity to draw the attention of others outside the field of geotechnical engineering to the importance of what we are doing, particularly to those who, directly or indirectly, rely on our services, knowledge and experience. Investment in quality geotech-

nical work is required for successful and safe design, construction and operation of any infrastructure. Geotechnical engineering is the key to a safe and sustainable infrastructure and of importance for the society, economy and the environment. This must be emphasized and reported upon.



**XVI Asian Regional Conference on
Soil Mechanics and Geotechnical Engineering
"Geotechnique for Sustainable Developments
and Emerging Market Regions"
21 - 25 October 2019, Taipei, China
www.16arc.org**



**PANAMERICANO 2019
Cancun Mex.**

**XVI Panamerican Conference on Soil Mechanics
and Geotechnical Engineering
18-22 November 2019, Cancun, Quintana Roo, Mexico
<http://panamerican2019mexico.com/panamerican>**

Conference Topics

- Laboratory and in situ testing
- Analytical and physical modelling in geotechnics
- Numerical modelling in geotechnics
- Unsaturated soils
- Soft soils.
- Foundations and retaining structures
- Excavations and tunnels
- Offshore
- Transportation in geotechnics
- Natural hazards
- Embankments, dams and tailings
- Soils dynamics and earthquake engineering
- Ground improvement
- Optimizing Construction and Sustainable Development
- Preservation of historic sites
- Regulations and Innovation
- Rock mechanics
- Education

Contact Info

Bldv. Kukulcan Km 17, Zona Hotelera,
77500 Cancún, QROO
Tel (+52) 1 55 5677-3730, (+52) 1 55 5679-3676
Iberostar: 01 800 849 1047
info@panamerican2019mexico.com
chat@panamerican2019mexico.com



**Nordic Geotechnical Meeting
27-29 May 2020, Helsinki, Finland**

Contact person: Prof. Leena Korkiala-Tanttu
Address: SGY-Finnish Geotechnical Society,
Phone: +358-(0)50 312 4775
Email: leena.korkiala-tanttu@aalto.fi

10 of the world's greatest tunnels

Gotthard Base Tunnel (Switzerland)



European leaders including German Chancellor Angela Merkel and French President Francois Hollande turned out for the Gotthard's Base Tunnel's grand opening in June, which featured colorful and often surreal scenes involving costumed dancers, fireworks and plenty of yodeling.

Reaching a depth of 2,300 meters (7,545 feet, almost 1.5 miles) the tunnel will slice an hour off travel time between Zurich, Switzerland, and Milan, Italy.

The 57-kilometer tunnel runs between the towns of Erstfeld in the north and Bodio in the south.

Trains reaching speeds of up to 250 kilometers an hour (155 mph) can travel through in 20 minutes, according to the Swiss Travel System.

Normal commercial traffic began in earnest on December 11, when the first regular passenger train left Zurich at 6.09 a.m. local time and arrived in Lugano at 8.17 a.m.

Gotthard overtakes the 53.9-kilometer Seikan Tunnel in northern Japan as the longest rail tunnel in the world and relegates the 50.5-kilometer Channel Tunnel between Britain and France into third place.

Length: 57 kilometers (35 miles)

Fast fact: 3,200 kilometers of copper cable was used in the tunnel's construction -- enough to stretch from Madrid to Moscow.

More info: [Gotthard Base Tunnel](#)

Channel Tunnel (UK and France)

Connecting the United Kingdom with continental Europe (it has entrances/exits in Folkestone, Kent, and Pas-de-Calais in northern France), the tunnel has the world's longest under-sea section -- 37.9 kilometers (23.5 miles).

Though a marvel of the modern age, it wasn't a new idea when it was built.

French engineer Albert Mathieu proposed a tunnel under the English Channel in 1802, although his plans included an

artificial island mid-channel where horse-drawn carriages could make maintenance stops.



"This tunnel defined the term 'mega project,'" says Matt Sykes, tunnel expert and director at engineering company Arup.

"It fundamentally changed the geography of Europe and helped to reinforce high speed rail as a viable alternative to short-haul flights."

Length: 50 kilometers (31 miles)

Fast fact: Though both the English and French put in work to build the Channel Tunnel, the English side tunneled a greater distance.

More info: [Eurotunnel](#)

Laerdal Tunnel (Aurland, Norway)



The Laerdal Tunnel in West Norway is the world's longest road tunnel and cost \$153 million to build, which works out at \$6,250 per meter.

The length of the tunnel prompted engineers to include various features designed to alleviate claustrophobia and tiredness.

"The sheer length of tunnel -- which takes 20 minutes to drive through -- led to innovation in the use of behavioral science and driver psychology in the design to reduce driver fatigue and improve safety," says Sykes.

"This resulted in large, colorfully lit caverns every six kilometers, providing points of interest and a unique driver experience."

Length: 24.5 kilometers (15.2 miles)

Fast fact: Engineers separated the tunnel into different sections to give the illusion that drivers are traveling through a number of smaller tunnels.

In these smaller sections drivers can take breaks, or even have a wedding ceremony, as one adventurous couple has previously done.

More info: [Laerdalstunnelen](#)

Tokyo Bay Aqua-Line (Tokyo)



Tokyo's Aqua-Line: Bridge above, tunnel beneath.

It's easy to mistake this tunnel for a bridge because part of the structure comprises a 4.4-kilometer span as well as a 9.6-kilometer subsea conduit.

The Aqua Line crosses Tokyo Bay and connects the cities of Kawasaki and Kisarazu.

It reduced the journey time between the two from 90 to 15 minutes.

"This project required the world's largest undersea tunnel boring machines and set the precedent for constructing two-lane road tunnels," points out Matt Sykes at Arup.

"The resilience of the construction was demonstrated during the 2011 Tohoku-Pacific Ocean earthquake, which caused severe damage to Tokyo Bay."

Length: 14 kilometers total (8.7 miles)

Fast fact: Constructed atop the Tokyo Bay Aqua Line is an island that functions as a rest area and mall.

The man-made island, called Umi-Hotaru, is a popular scenic point with an observation deck that gives a great view of Tokyo Bay.

More info: [Nippon Civil Consulting Engineers](#)

Eisenhower Tunnel (Colorado)



Colorado's Eisenhower road tunnel is one of the world's highest, located 3,401 meters (11,158 feet) above sea level.

el, at the highest point on the U.S. interstate highway system.

It played a significant role in the women's rights movement when Janet Bonnema was hired as a construction worker in 1972.

Her supervisor misread her name as James, but realized his mistake and reassigned her to administrative duties after workers -- many of whom were former miners -- cited the common superstition that a woman's presence can bring bad luck to a mine.

Bonnema sued and was allowed to return to the tunnel.

A new equal rights law was subsequently passed.

Length: 2.72 kilometers (1.7 miles)

Fast fact: Prior to the tunnel's official opening in 1972, a drunk driver believed he should be the first person to take a vehicle through and was arrested for trespassing.

Charges were subsequently dropped because the signs prohibiting traffic were considered inadequate.

More info: [Colorado Department of Transportation](#)

Spiralen Tunnel (Drammen, Norway)



The dramatic Spiralen road tunnel, built in 1961 and comprising six spirals covering 1,649 meters (5,413 feet), leads to one of the most spectacular viewpoints in the industrial town of Drammen.

"Despite being an expensive country, Norway builds some of the cheapest tunnels," says Alun Thomas, head of tunnels at engineering consultancy Ramboll.

"This is because the engineers strip the design down to the bare essentials required for the flow of traffic in the tunnels. Maximum benefit for minimum effort -- that's good engineering."

Length: 1.65 kilometers (1.02 miles)

Fast fact: The tunnel opens out to a dramatic view of Drammen Valley and has a beer garden, restaurants and open-air museum.

More info: [Spiralen in Drammen](#)

Guoliang Tunnel (Henan Province, China)

Before the construction of this impressive tunnel, the only way to access the village of Guoliang was via a narrow path carved into the side of the Taihang Mountains.

In 1972, a group of 13 villagers decided to construct a tunnel, which they dug by hand.

Three died during the construction process but the tunnel transformed the village and became a tourist attraction in its own right.

"This tunnel is beautiful and a tribute to the tenacity of the villagers who built it," says Thomas at Ramboll.

"For me it emphasizes how tunnel construction can enhance the environment as well as bringing huge benefits for society. At the same time, one should remember the cost and the fact that several villagers were killed during construction."

Length: 1.2 kilometers (0.74 miles)

Fast fact: The tunnel was built jagged and steep due to the village's primitive tools, earning it the nickname: "The road that does not tolerate any mistakes."

SMART (Kuala Lumpur, Malaysia)



"SMART is a combined road and flood relief tunnel," explains Thomas at Ramboll.

"It can be completely flooded to get rid of storm water and turned back into a road in a few hours."

The tunnel, the longest in Malaysia, was built to solve the problem of flash flooding in Kuala Lumpur.

SMART can operate in three ways.

When there's no flooding, it serves purely as a road tunnel.

When there are floods, rainwater can be diverted into a lower channel, and the upper level will remain open to traffic.

When exceptionally heavy floods occur, the tunnel closes to all traffic and watertight gates open to allow floodwater to flow through.

Length: 9.7 kilometers (6.02 miles)

Fast fact: The tunnel is expected to prevent billions of dollars of possible flood damage and costs from traffic congestion.

Since it opened in 2007, flood-prone areas such as Masjid Jamek, Dataran Merdeka, Leboh Ampang and Jalan Melaka have been spared inundation.

More info: [SMART Motorway Tunnel](#)

Bund Sightseeing Tunnel (Shanghai)



This underwater Chinese tunnel is short and sweet, but spectacular and slightly strange.

It spans the Huangpu River and connects Shanghai's Bund to Lujiazui, location of the Pearl TV tower.

Passengers were originally going to be ferried from one side to the other on a moving walkway, but automated cars were installed instead.

Length: 646.7 meters (2,122 feet)

Fast fact: A company that had worked with Disney was originally supposed to help design the tunnel, but was deemed too expensive.

Instead a Shanghai-based company created the tunnel's psychedelic lights and trippy audio-visual effects.

The ride is apparently meant to represent a journey to the core of the earth.

Seikan Tunnel (Japan)

The Seikan is a railway tunnel in Japan, but what makes it unique is the fact that a 23-kilometer (14.2 miles) stretch of the tunnel is 140 meters (460 feet) below sea level.

Until the Gotthard Base Tunnel came along, it was the longest and deepest rail tunnel in the world.

It spans the Tsugaru Strait, connecting Aomori Prefecture on the island of Honshu to the island of Hokkaido.

Work on the tunnel started in 1964 and was completed in 1988.

Length: 53 kilometers (32.9 miles)

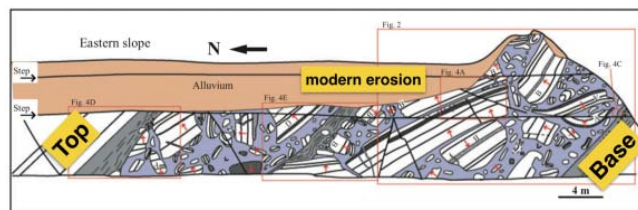
Fast fact: In 1976, construction workers hit a patch of soft rock and water gushed into the tunnel at a rate of 80 tons per minute. The leak took two months to fix.

More info: [JR-Hokkaido Hakadote Branch](#)

(CNN's Tim Hume, Hilary Whiteman, George Webster, Tamara Hinson, Sofia Couceiro and Maureen O'Hare contributed to this report, December 12, 2016, <http://edition.cnn.com/2016/12/12/travel/great-tunnels-2016/>)



Submarine landslide deposits – a spectacular outcrop example from Japan



Here is another nice photo from a [field symposium web-site](#) showing a closeup of the deposit.

(<https://offtheshelfedge.wordpress.com/>)

I tweeted an image that got a lot of attention the other day and wanted to follow it up with a quick post describing the deposit. The back story is this: [Lesli Wood](#), a submarine landslide expert, showed an image at a recent conference that is a spectacular example of a mass transport deposit (MTD), or more simply, a submarine landslide deposit.

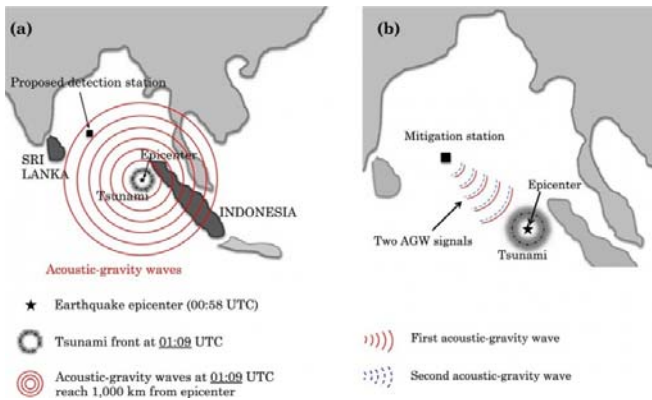
Landslides occur on land ([example video](#)), causing plenty of infrastructure damage and other problems. While they are difficult to view and visualize, landslides also occur on the seafloor, causing massive reorganization of the seafloor that can generate tsunamis. In fact, the [Storegga slide](#) that occurred offshore Norway about 6000 B.C. likely killed many Europeans.



Due to their volume and size, submarine landslides are usually characterized best with seismic reflection data – the map and cross section below from [this paper by T.M. Alves](#). The map shows large blocks of rock that have been broken apart and transported downslope (from left to right) and the cross section shows what the internal character of those blocks are. Note the discordant nature of the blocks, very similar to the image above of the outcrop, with rocks in all directions.

Outcrops usually are too small or not well enough exposed to view these types of features, but the outcrops created by road making on the Boso Peninsula in Japan are definitely good enough. This paper by [Yamamoto et al](#) (download the paper [here](#)) describing these outcrops has a very nicely drawn diagram that demonstrates the deposit. There are probably two landslide deposits that are stacked here, with a turbidite separating them (grey layer in the middle of the diagram).

Cardiff researcher proposes anti-tsunami concept Sound waves could be used to dissipate the energy of tsunamis and potentially save lives, according to a researcher from Cardiff University.



In the journal *Heliyon* (<http://www.heliyon.com/article/e00234>), Dr Usama Kadri, from the university's School of Mathematics, outlines how acoustic-gravity waves (AGWs) could be fired at a tsunami to reduce its amplitude, or height. AGWs are natural sound waves that travel in the oceans, sometimes thousands of metres below the surface. If we could find a way to engineer these waves, we could use them to diminish the energy of tsunamis and protect populations living in coastal areas.

The proposed system would involve two AGWs fired at the tsunami's epicentre to form what's known as a resonant triad. Research suggests that mitigation of surface gravity waves (tsunamis) is possible through a careful resonant triad interaction.

"Within the last two decades, tsunamis have been responsible for the loss of almost half a million lives, widespread long-lasting destruction, profound environmental effects and global financial crisis," said Dr Kadri.

"Up until now, little attention has been paid to trying to mitigate tsunamis and the potential of acoustic-gravity waves remains largely unexplored."

The 2004 Boxing Day tsunami killed over 230,000 people in 14 countries, and the energy released by the earthquake that caused it was estimated to be the equivalent of approximately 1,500 Hiroshima bombs. In order to use AGWs in tsunami mitigation, engineers would first need to develop highly accurate AGW frequency transmitters or modulators, which Dr Kadri admits would be difficult.

"In practice, generating the appropriate acoustic-gravity waves introduces serious challenges due to the high energy required for an effective interaction with a tsunami," he explained.

"However, this study has provided proof-of-concept that devastating tsunamis could be mitigated by using acoustic-gravity waves to redistribute the huge amounts of energy stored within the wave, potentially saving lives and billions of pounds worth of damage."

ΕΝΔΙΑΦΕΡΟΝΤΑ - ΛΟΙΠΑ

Η ψηλότερη γέφυρα του κόσμου



Λίγες μέρες πριν αλλάξει η χρονιά, μία ακόμα θαυμαστική κατασκευή ήρθε να προστεθεί στον μακρύ κατάλογο με τα αρχιτεκτονικά επιτεύγματα της Κίνας.

Ο λόγος για τη γέφυρα Beipanjiang, η οποία χτίστηκε σε υψόμετρο 565 μ. και είναι η ψηλότερη του κόσμου.

Βρίσκεται σε ένα απομακρυσμένο σημείο της επαρχίας Guizhou, στα νότια της χώρας, και αναμένεται να αποδειχτεί σωτήρια για τους ντόπιους, οι οποίοι θα γλιτώσουν πολύτιμο χρόνο στις μετακινήσεις τους, αφού η απόσταση ανάμεσα στις πόλεις Xuanwei και Liuranshui μειώνεται από πέντε σε μόλις δύο ώρες!

Η νεότευκτη γέφυρα αποτελείται από τέσσερις λωρίδες κυκλοφορίας, έχει κύριο άνοιγμα μήκους 720 μ., ενώ από κάτω της κυλάει ο ποταμός Beipan.

(Ελευθερία Αλαβάνου / Η ΚΑΘΗΜΕΡΙΝΗ, 16.01.2017
<http://www.kathimerini.gr/891607/article/ta3idia/ta3idiwtika-nea/h-yhloterh-gefyra-toy-kosmoy>)



Roman Arch Bridges: How much weight can they hold and how did they last so long?



At the core of the Roman Empire was their engineering prowess, and most notable of all their infrastructure advances was the roman arch.

The arch bridge and arched structures allowed the Romans to construct buildings with a far greater ratio of wall openings to height than had ever been possible before. The evidence of such architecture is found in not only the Roman Coliseum but also the labyrinth of arched catacombs that lie beneath historic Rome. Focusing in on the arch bridge, it was a technology never seen before, one that allowed boats to pass under walkways and roads and one that enabled the Roman's famous series of raised aqueducts.

Why was the arched bridge so crucial to the roman empire, and what structural properties of the arch have that enabled roman architecture to survive relatively in-tact even to modern times?

An arch bridge was, and is, so revolutionary to structural design because the elements of which function almost entirely in compression. Due to the distribution of both dead and live loads on arches, stresses are always translated in compression, allowing for materials such as rock, or unreinforced concrete, to be used effectively. If you know anything about concrete's and rock's material strengths, you likely know that neither function practically in tension loading. Nowadays, concrete beams are reinforced with rebar to allow for tension loading, but the Romans didn't have that ability.

As an arch's radius of curvature increases, it begins to behave slightly more like a beam, therefore low compression forces or tension forces, begin to appear on the underside of the arch. The Pantheon, still the biggest unreinforced concrete dome structure in existence is estimated to have been the largest domed structure the Roman's could have built without collapse.



Pont Julien, a 3 BC Roman arch bridge over the Calavon river, built on the Via Domitia, France

Examining how much load an arched bridge can hold is a little tricky. Since all of the components of an arch function in compression loading, the maximum loading values of any given arch is essentially equivalent to the shearing point of any material. Granite, for example, would be a far better arch construction material than sandstone. Even still, the ability for arches to hold load is far beyond any other structural element, even those today.

A well-built arch from stone doesn't even need mortar to connect the parts, rather the friction forces from compression keep the structure stable. Rather than spend hours determining the maximum load of an arch constructed from a given stone, we are going to settle with a maximum loading value of a really big number. For the Romans, and even engineer's today, a *solid* arch structure's yield point is far beyond realistic loads that structure would ever see.

These same principles that made the arch so strong also made them last so long. When a structure created from arches undergoes a series of loads creating low material stresses and strains, fatigue seen in the arch over time is very minimal, if nothing. Since arch's yield points are so far beyond practical loading values, they tend to last until the rock or structure is weathered. In turn, a very long time.



The Pont du Gard aqueduct is as old as the Christian religion

The Romans did use concrete to build many of their structures, like the Coliseum, which is known to be about 10 times weaker than modern concrete. However, while the concrete was weaker, it was far more resistant to weathering than modern concrete due to the abundance of volcanic ash used in its construction. Through this increased weathering capabilities and the strength of solid arch structures, Roman architecture and buildings are still around today, in nearly all of their original beauty.

Sources: [Smithsonian](http://www.smithsonianmag.com/history/the-secrets-of-ancient-romes-buildings-234992/?no-ist) (<http://www.smithsonianmag.com/history/the-secrets-of-ancient-romes-buildings-234992/?no-ist>), [Hesston, How Stuff Works](http://www.howstuffworks.com/engineering/civil/bridge5.htm) (<http://www.howstuffworks.com/engineering/civil/bridge5.htm>)

(Trevor English / THE SHORT SLEEVE AND TIE CLUB, January 16, 2017, <http://shortsleeveandtieclub.com/roman-arch-bridges-how-much-weight-can-they-hold-and-how-did-they-last-so-long>)

(<http://www.howstuffworks.com/engineering/civil/bridge5.htm>)



Elbphilharmonie: το νέο μουσικο-αρχιτεκτονικό θαύμα της Ευρώπης

Ήταν ένα από τα πιο αναμενόμενα νέα εμβληματικά κτίρια της Ευρώπης. Οι κάτοικοι του Αμβούργου το περίμεναν για χρόνια. Εγκαινιάστηκε χθες, στο Hafen City, στην περιοχή που αποτελεί το ορόσημο της πόλης τα τελευταία χρόνια.

Σήμερα, μία μέρα μετά από τα επίσημα εγκαινιά του να προκαλεί δέος κατορθώνοντας και κάνοντας όλα του τα μελλοντικά γεγονότα να γίνονται sold out το ένα μετά από το άλλο. Όλα αυτά για το αρχιτεκτονικό θαύμα του ολοκαίνουριου Μεγάρου Μουσικής στο Αμβούργο. Ένα κτίριο σταθμό στην πολιτιστική και ταυτόχρονα αρχιτεκτονική σκηνή, τόσο της Ευρώπης όσο και διεθνώς.



Φέρει την αρχιτεκτονική υπογραφή των **Herzog & de Meuron** και αποτελεί το ψηλότερο επισκέψιμο κτίριο σε όλο το Αμβούργο. Χτισμένο πάνω στον ποταμό Elbe στην περιοχή του Hafen City, το Elbe Philharmonic Hall (η επίσημη ονομασία του στην αγγλική) αποτελεί ένα από τα μεγαλύτερα και πλέον προνομιούχα όσο αφορά την ακουστική τους μέγαρα μουσικής παγκοσμίως.



Η κατασκευή του από γυαλί με το σχέδιό του να θυμίζει ένα κύμα νερού υψωμένο στα 110 μέτρα ύψος πάνω από μια αποθήκη του 1963 κοντά στην ιστορική Speicherstadt. Η κατασκευή ξεκίνησε το 2007 και αρχικός προϋπολογισμός ήθελε το κόστος ανέγερσής του να φτάνει τα 450 εκατομμ. ευρώ. Παραδόθηκε το 2016 όταν και έγινε η πρώτη επίσημη δοκιμή του. Με μεγάλη καθυστέρηση και μεγάλη υπέρβαση προϋπολογισμού που λένε ότι θα ξεπεράσει κατά πέντε φορές την αρχική πρόβλεψη. Η συζήτηση που προκάλεσε η αργοπορία του είναι παροιμιώδης για τη Γερμανία. Το δυτικότερο τμήμα του κτιρίου νοικιάζεται από την Westin αποτελώντας ουσιαστικό το Westin Hamburg Hotel φιλοξενώντας 45 δωμάτια.

Το τελικό του κόστος ανέρχεται πλέον στα 789 εκατομ. ευρώ. Στις 11 Ιανουαρίου 2017 το Elbphilharmonie εγκαινιάζεται επίσημα με ένα μεγάλο κονσέρτο της ορχήστρας NDR Elbphilharmonie υπό την διεύθυνση του Thomas Hengelbrock. Το πρόγραμμά του γεμάτο σπουδαίες και υποσχόμενες παραστάσεις με το κοινό να τις μετατρέπει ήδη σε sold out.

Το Elbphilharmonie είναι ένα αρχιτεκτονικό θαύμα

Πρόκειται για ένα απόλυτο, συνολικό, αρχιτεκτονικό έργο τέχνης. Συνδυάζει καινοτόμα αρχιτεκτονική σε μια ιδιαίτερη τοποθεσία, με την πλέον σύγχρονη ακουστική παγκοσμίως αλλά και επί της ουσίας του ένα οραματικό μουσικό πρόγραμμα. Το Elbphilharmonie με την εντυπωσιακή πρόσοψη από γυαλί που κόβει την ανάσα, κρύβει στο εσωτερικό του δύο αίθουσες συναυλιών και ένα ξενοδοχείο με διαμερίσματα αλλά και ένα μεγάλο φουαγιέ που οδηγεί στην plaza. Η plaza εκτείνεται ανάμεσα στην παλιά αποθήκη του 1963 και την γυάλινη κατασκευή, ως δημόσιο πεδίο θέασης 360 μοιρών στην πόλη ενώ στο "The Grand Hall", την καρδιά του Elbphilharmonie, υπάρχει χωρητικότητα 2.100 επισκεπτών.

Το καθοριστικό χαρακτηριστικό του Elbphilharmonie δεν είναι άλλο από το γυαλί. Για το εντυπωσιακό κύμα χρειάστηκαν 1.000 κυρτά παράθυρα πάνελ, tailor-made έτσι ώστε να αιχμαλωτίζουν και να αντανακλούν το χρώμα του ουρανού, τις ακτίνες του ήλιου, το νερό και την πόλη μετατρέποντας το Μέγαρο Μουσικής σε ένα γιγαντιαίο κρύσταλλο.

Η αρχιτεκτονική αισθητική γραμμή άλλωστε ορίζεται με σαφήνεια ακόμα και από το Φουαγιέ του κτιρίου που οδηγεί στην Grand Hall αίθουσα. Οι πολυεπίπεδες σκάλες, περικυκλώνουν την αίθουσα συναυλιών ευρύχωρα, δημιουργώντας εντυπωσιακά εφέ φωτισμού και προσφέροντας εκπληκτική θέα στην πόλη, στον ποταμό Έλβα και το λιμάνι από κάθε επίπεδο του φουαγιέ.

Με ακουστική τελευταίας γενιάς

Υπεύθυνος για την εξαιρετική ακουστική του χώρου ο διάσημος Ιάπωνας Yasuhisa. Στόχος της εταιρείας Toyoτα του διάσημου Ιάπωνα, για την αίθουσα Grand Hall ήταν η αίθουσα να ενισχύει την φυσική ακουστική της μουσικής, αλλά και να είναι ευαίσθητη σε ηλεκτρονικά συστήματα ήχου. Με αυτόν τον τρόπο, το κοινό μπορεί επίσης να απολαύσει μέχρι και ροκ συναυλίες στο Elbphilharmonie. Η Toyoτα πιστεύει ότι το Elbphilharmonie άλλωστε πλέον συγκαταλέγεται μεταξύ των καλύτερων αιθουσών συναυλιών στον κόσμο ως προς την ακουστική του.



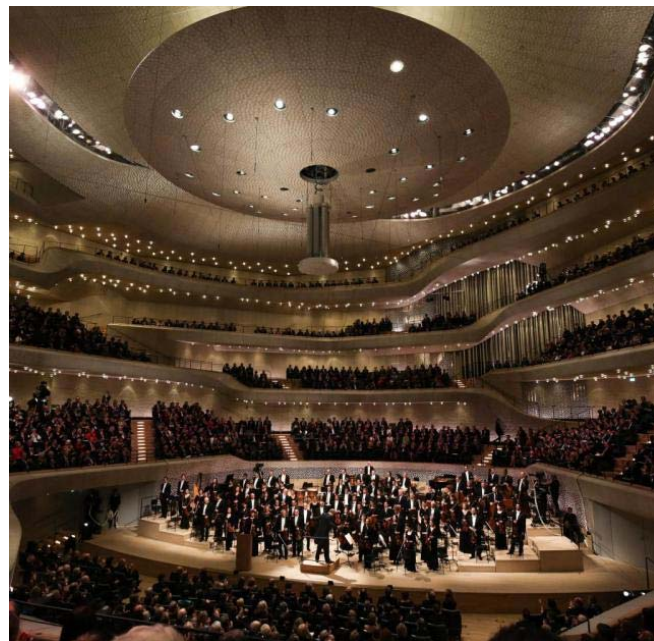
Οι αρχιτέκτονες του θαύματος

Οι αρχιτέκτονες Pierre de Meuron, Jacques Herzog και Ascan Mergenthaler εργάζονται πάνω στο πρότζεκτ του Elbphilharmonie από το 2003. Το αρχιτεκτονικό τους γραφείο ως "Herzog and de Meuron" ιδρύθηκε στο Basel το 1978. Στο πορτφόλιό τους μετράνε μεγάλα και σημαντικά έργα, όπως η Tate Modern στο Λονδίνο, το Alliance Arena στο

Μόναχο και το Εθνικό Στάδιο του Πεκίνου για τους Ολυμπιακούς Αγώνες του 2008.

Το σημείο είναι άκρως συμβολικό

Η μουσική, το μέλλον και η Τέχνη ανθίζει σε μία παραδοσιακά εργατική περιοχή του Αμβούργου. Το Elbphilharmonie τοποθετείται στο ιστορικό Sandtorhafen, το παλιό λιμάνι εργασίας του Αμβούργου για αιώνες. Η Kaiserspeicher, η μεγαλύτερη αποθήκη του Αμβούργου μέσα στο νερό, χτίστηκε το 1875. Καταστράφηκε τον Δεύτερο Παγκόσμιο Πόλεμο όταν ανοικοδομήθηκε, μετονομάστηκε σε Kaispeicher. Εκεί ακριβώς που πλέον βρίσκουμε το εντυπωσιακό Μέγαρο.



Με θέα 360 μοίρες σε όλη την περιοχή

Σε ύψος 37 μέτρων πάνω από το επίπεδο του εδάφους, η δημόσια "πλατεία" θέασης που δημιουργείται ανάμεσα στην αποθήκη και την πρόσοψη, προσφέρει στους επισκέπτες την δυνατότητα μιας εκπληκτικής 360 ° θέας στην πόλη και το λιμάνι. Η πλατεία είναι ανοιχτή στους πολίτες του Αμβούργου, σε τουρίστες, στους επισκέπτες του ξενοδοχείου καθώς όλοι είναι ευπρόσδεκτοι να κάνουν μια βόλτα κατά μήκος αυτής της μοναδικής "διάβασης".



(Από [parallaxi](http://parallaximag.gr/life/texnes/elbphilharmonieneo-mousiko-architektoniko-thavma-tis-evropis) - January 12, 2017, <http://parallaximag.gr/life/texnes/elbphilharmonieneo-mousiko-architektoniko-thavma-tis-evropis>)



www.geoengineer.org

Κυκλοφόρησε το Τεύχος #141 του **Newsletter του Geo-engineer.org** (Ιανουαρίου 2017) με πολλές χρήσιμες πληροφορίες για όλα τα θέματα της γεωμηχανικής. Υπενθυμίζεται ότι το Newsletter εκδίδεται από τον συνάδελφο και μέλος της ΕΕΕΕΓΜ Δημήτρη Ζέκκο (secretariat@geoengineer.org).

Ενδεικτικά αναφέρονται:

- Landslide in Greece cuts off access to an entire village (video)
- Direct and residual shear testing of undisturbed and remolded soil samples
- New Zealand Kaikoura 7.8M Earthquake Reconnaissance Efforts Take Advantage of Drone and 3D Mapping Technology
- Giant sinkhole opens up in Northern Cape, South Africa (Video)
- Watch the video performance of GeoConcrete® Column System by Geopier
- Avalanche triggered by quakes buries hotel in Italy
- Washington employs LiDAR technology against landslide risk
- Channel Slab Pile CAP Assemblies by Hubbell
- The updated FHWA Deep Foundation Load Test Database (DFLTD v.2) is now available!
- Curtis High School Addition and Renovation Project, a project milestone
- Did Mount Everest shrink after the 2015 Nepal quake?
- Humboldt: Power Mechanical Earth Drill
- Massive Landslide Strikes Northern Argentina
- ISSMGE Case Histories Journal publishes Vol. 4, Issue 1. Access here!
- Geotechnical software for lab data management

<http://campaign.r20.constantcontact.com/render?m=1101304736672&ca=db8532af-91dc-49c6-8d18-9ea38eced1d5>



Dear ISRM Member

The Volume 19, December 2016 issue of the ISRM News Journal is now online on the ISRM website. Since 2012 the ISRM distributes the News Journal to all members in electronic version, and prints copies which are available at our sponsored symposia.



The News Journal includes news from the society life, including board and regional reports, commission work, conference and symposia reports and papers from awarded members, among other content. [Click here to read it directly on our website or to download it.](#)

Best regards

Luís Lamas
ISRM Secretary General

ΕΚΤΕΛΕΣΤΙΚΗ ΕΠΙΤΡΟΠΗ ΕΕΕΕΓΜ (2015 – 2018)

Πρόεδρος	:	Γεώργιος ΓΚΑΖΕΤΑΣ, Δρ. Πολιτικός Μηχανικός, Καθηγητής Ε.Μ.Π. president@hssmge.gr , gazetas@ath.forthnet.gr
Α΄ Αντιπρόεδρος	:	Παναγιώτης ΒΕΤΤΑΣ, Πολιτικός Μηχανικός, ΟΜΙΛΟΣ ΤΕΧΝΙΚΩΝ ΜΕΛΕΤΩΝ Α.Ε. otmate@otenet.gr
Β΄ Αντιπρόεδρος	:	Μιχάλης ΠΑΧΑΚΗΣ, Πολιτικός Μηχανικός mpax46@otenet.gr
Γενικός Γραμματέας:		Μιχάλης ΜΠΑΡΔΑΝΗΣ, Πολιτικός Μηχανικός, ΕΔΑΦΟΣ ΣΥΜΒΟΥΛΟΙ ΜΗΧΑΝΙΚΟΙ Α.Ε. mbardanis@edafos.gr , lab@edafos.gr
Ταμίας	:	Γιώργος ΝΤΟΥΛΗΣ, Πολιτικός Μηχανικός, ΕΔΑΦΟΜΗΧΑΝΙΚΗ Α.Ε.- ΓΕΩΤΕΧΝΙΚΕΣ ΜΕΛΕΤΕΣ Α.Ε. gdoulis@edafomichaniki.gr
Έφορος	:	Γιώργος ΜΠΕΛΟΚΑΣ, Δρ. Πολιτικός Μηχανικός, Επίκουρος Καθηγητής ΤΕΙ Αθήνας gbelokas@teiath.gr , gbelokas@gmail.com
Μέλη	:	Ανδρέας ΑΝΑΓΝΩΣΤΟΠΟΥΛΟΣ, Δρ. Πολιτικός Μηχανικός, Ομότιμος Καθηγητής ΕΜΠ aanagn@central.ntua.grn Βάλια ΞΕΝΑΚΗ, Δρ. Πολιτικός Μηχανικός, ΕΔΑΦΟΜΗΧΑΝΙΚΗ Α.Ε. vxenaki@edafomichaniki.gr Μαρίνα ΠΑΝΤΑΖΙΔΟΥ, Δρ. Πολιτικός Μηχανικός, Αναπληρώτρια Καθηγήτρια Ε.Μ.Π. mpanta@central.ntua.gr
Αναπληρωματικό Μέλος	:	Κωνσταντίνος ΙΩΑΝΝΙΔΗΣ, Πολιτικός Μηχανικός, ΕΔΑΦΟΜΗΧΑΝΙΚΗ Α.Ε. kioannidis@edafomichaniki.gr
Εκδότης	:	Χρήστος ΤΣΑΤΣΑΝΙΦΟΣ, Δρ. Πολιτικός Μηχανικός, ΠΑΝΓΑΙΑ ΣΥΜΒΟΥΛΟΙ ΜΗΧΑΝΙΚΟΙ Ε.Π.Ε. editor@hssmge.gr , ctsatsanifos@pangaea.gr

ΕΕΕΕΓΜ

Τομέας Γεωτεχνικής
ΣΧΟΛΗ ΠΟΛΙΤΙΚΩΝ ΜΗΧΑΝΙΚΩΝ
ΕΘΝΙΚΟΥ ΜΕΤΣΟΒΙΟΥ ΠΟΛΥΤΕΧΝΕΙΟΥ
Πολυτεχνειούπολη Ζωγράφου
15780 ΖΩΓΡΑΦΟΥ

Τηλ. 210.7723434
Τοτ. 210.7723428
Ηλ-Δι. secretariat@hssmge.gr ,
geotech@central.ntua.gr
Ιστοσελίδα www.hssmge.org (υπό κατασκευή)

«ΤΑ ΝΕΑ ΤΗΣ ΕΕΕΕΓΜ» Εκδότης: Χρήστος Τσατσανίφος, τηλ. 210.6929484, τοτ. 210.6928137, ηλ-δι. ctsatsanifos@pangaea.gr,
editor@hssmge.gr, info@pangaea.gr

«ΤΑ ΝΕΑ ΤΗΣ ΕΕΕΕΓΜ» «αναρτώνται» και στην ιστοσελίδα www.hssmge.gr